Glacial to deglacial reservoir ages of surface waters in the southern South Pacific

Kevin Küssner[1)], Michael Sarnthein[2)], Frank Lamy[1)], Elisabeth Michel[3)], Gesine Mollenhauer[1)], Thomas A. Ronge[1)], Giuseppe Siani[4)], and Ralf Tiedemann[1]

Affiliations:

1) Alfred-Wegener-Institut Helmholtz-Zentrum für Polar- und Meeresforschung, Department for Marine Geology, 27570 Bremerhaven, Germany, kevin.kuessner@awi.de, frank.lamy@awi.de, Gesine.Mollenhauer@awi.de, <Thomas.Ronge@awi.de>, ralf.tiedemann@awi.de,

2) Institute of Geosciences, University of Kiel, Olshausenstr. 40, 24098 Kiel, Germany, michael.sarnthein@ifg.uni-kiel.de, (corresponding author)

3) LSCE-IPSL, CNRS-CEA-UVSQ Bât 714, L'Orme des Merisiers, 91191 Gif-sur-Yvette Cedex, France, Elisabeth.Michel@lsce.ipsl.fr,

4) Laboratoire GEOPS UMR 8148, CNRS-Université Paris Saclay, Département des Sciences de la Terre, Bât. 504 (RdC), 91405 ORSAY Cedex, France, giuseppe.siani@u-psud.fr,

Plain Language Summary

This study is focused on the time coordinate of paleoclimate research. It employs an advanced tuning technique to age-classify glacial-to-deglacial ocean sediments with semi-millennial resolution and a new level in dating accuracy. The method is based on age-calibrated suites of atmospheric radiocarbon plateaus that are reflected by analogous radiocarbon plateaus obtained from planktic foraminifers sampled in sediment cores at centennial-scale resolution. The results provide a novel record of short-term changes in the radiocarbon age of dissolved carbon and ventilation, i.e. the 'reservoir age' of ocean surface waters. Such proxy records document variations in ocean circulation and mixing, now established at four sites along the western and eastern margins of the subpolar South Pacific. The age tie points are confirmed in a sediment core off Chile by independently dated marine ash layers. Our results provide precise stratigraphic correlations across the ocean and with paleoclimate records of Antarctic ice cores. In particular, the age records support the model of "bipolar seesaw" at the onset of rapid deglacial Antarctic warming coeval with the onset of the Heinrich cold spell in the North Atlantic, moreover, with the Antarctic Cold Reversal that preceded the onset of the Younger Dryas cold spell in the northern Hemisphere.

Abstract

Ocean sediment records document abrupt changes in glacial-to-deglacial circulation and mixing of the ocean, recorded as changes in ^{14}C reservoir ages of surface waters. Here we present ^{14}C-based high-resolution age records of four sediment cores derived by means of ^{14}C plateau tuning. This provides a detailed and precise stratigraphic correlation between the western and eastern South Pacific and paleoclimate records of Antarctic ice cores as well as ^{14}C reservoir ages. The accuracy and precision of plateau tuning are confirmed in two sediment cores off Chile; in one core by independent land-based age control of four tephra layers, in a second core by a suite of glacial sediment varves. During glacial times, high reservoir ages reaching up to ~1500 yr may reflect seasonal sea ice and/or a melt water lid at high latitudes both east of New Zealand and off southern Chile and may be linked to northward advection of upwelled old subsurface waters from the Polar Frontal Zone. Our results support the model of a bipolar seesaw at the onset of rapid deglacial Antarctic warming, moreover, they show that the Antarctic Cold Reversal immediately preceded the onset of the Younger Dryas cold spell.

Introduction

Glacial-to-interglacial changes in atmospheric pCO_2 are considered to be strongly affected by atmosphere-ocean mixing processes in the Southern Ocean. During the Last Glacial Maximum (LGM) a more extended and prolonged sea-ice cover, northward shifted Southern Hemisphere westerlies (Kohlfeld et al., 2013; Lamy et al., 2019), and reduced deep-water mixing (Skinner et al., 2015) led to an enhanced stratification of the deep Southern Ocean and reduced air-sea gas exchange (Sigman et al., 2010, Marcott et al., 2014) which implies a pronounced sequestration of CO_2 in circumpolar deep waters (e.g., Sarnthein et al., 2013; Ronge et al., 2016; 2020; Marzocchi and Jansen, 2019, Khatiwala, et al., 2019). The beginning of the last glacial termination in Antarctica at 17,600-17,800 calibrated years ago (17.6-17.8 cal. ka) (Kawamura et al., 2007; Buizert et al., 2018; Marcott et al., 2014) was linked to changes in overturning circulation of the deep Southern Ocean and a southward shift of the Southern Hemisphere westerlies (Denton et al., 2010; Toggweiler et al., 2006; Lamy, et al., 2007; Siani et al., 2013; Timmermann et al., 2014) that probably led to a southward shift of upwelling zones along the Antarctic Polar Frontal Zone and probably off western South America. These shifts went along with four distinct events of CO_2 outgassing (18.2-17.5; 17.4-16.7; 16.3-16.2; 14.75-14.53 cal. ka) from deep- ocean and permafrost reservoirs into the atmosphere as documented in Antarctic ice core records (Marcott et al., 2014). Events 1 and 2 paralleled a rapid drop in atmospheric $\delta^{13}C$ (Lourantou et al. 2010; Schmitt et al., 2012, Bronk Ramsey et al., 2012, Bauska et al., 2018) induced by an abrupt degassing of the deep ocean, also reflected by two atmospheric ^{14}C plateaus (Moy et al., 2019; Martinez-Fontaine et al., 2019; Sarnthein et al., 2020).

The knowledge of local ^{14}C reservoir ages, that is the difference between the ^{14}C age of marine surface waters and that of the contemporaneous atmosphere, is crucial to establish robust age control of past changes in surface and deep-water masses. Simple linear age correlations between ^{14}C based age tie points potentially contain large errors up to several hundred years, since they do not consider the numerous fast but significant temporal and spatial changes in ^{14}C concentration both of surface waters and the atmosphere (Sarnthein et al., 2015, 2020, accepted). Due to this lack of precision in centennial-scale age control the resulting age estimates in cal. years may hamper the quantification of the actual leads and lags, phasings and anti-phasings, and/or delayed response of proxy-based paleoceanographic signals compared to, for example, ice core and speleothem-based time series independent of ^{14}C dating. Accurate age relationships, however, are crucial for properly assessing the processes responsible for the shifts of carbon between different reservoirs.

On the basis of closely spaced age tie points surface water reservoir ages themselves may serve as a prime tracer to constrain past changes in surface water ventilation (Sarnthein et al. 2015, 2020; Balmer et al., 2016; Skinner et al., 2019). Reservoir/ventilation ages may provide intriguing insights into related changes in upwelling and stratification processes as well as in variations of local surface water productivity and the inventory of dissolved inorganic carbon (DIC). These insights may contribute to a better understanding of changes in atmospheric $\delta^{13}C$ that document the carbon release from the Ocean (Schmitt et al. 2012, Bauska et al. 2018).

The precise specification of temporal variations in ^{14}C reservoir ages is crucial for the global correlation of surface ocean changes such as sea surface temperature (SST) at centennial timescales and their link to terrestrial records including ice-cores (e.g., Pahnke et al., 2003, 2005; Lamy et al., 2007; De Pol-Holz et al., 2010; Martinez-Fontaine et al., 2019). Even at high sedimentation rates and high sampling resolution most records are hampered by the lack of narrow-standing tie points for absolute age control, and hence may fail to precisely constrain the timing of rapid changes in oceanography on centennial to millennial time scales. Previous chronologies that used age tie points such as a correlation of paleoclimate events to incremental time-scales of nearby ice cores (e.g., Pahnke et al., 2003) and/or that of independently dated ash layers (tephras) (Rose et al., 2010, Sikes et al., 2016) may suffer from a large uncertainty range of the age estimates, moreover, from their wide spacing of up to 5000 yr and more.

To circumvent this problem, more accurate ^{14}C-based correlation of paleoclimatic records can be achieved using a great number of robust tie points spaced over semi-millennials such as given by the narrow standing jump and plateau structures in the Suigetsu atmospheric ^{14}C record (Bronk Ramsey et al., 2012; Sarnthein et al., 2007, 2015, and 2020, accepted) in order to constrain regional reservoir age changes. Here we use this suite of atmospheric ^{14}C plateau boundaries as a reference record for global correlations reaching far beyond the tree ring-based evidence of the last 14 cal. ka, back to the base of the Last Glacial Maximum (LGM) near 27.5 cal. ka. In particular, we employ the technique of ^{14}C plateau tuning to four high-resolution sediment records from the western and two from the eastern continental margins of the South Pacific. In particular, sediment record MD07-3088 from the Chile continental Margin offers a unique opportunity to compare our ^{14}C plateau-based chronology to age estimates independently derived from four pre-Holocene tephra layers (Siani et al. 2013; Haddam et al., 2018).

The high-resolution chronology of four sediment cores from the Subantarctic South Pacific may help to constrain the following major objectives of paleoclimate research:

- To facilitate detailed temporal comparisons of paleoceanographic records to paleoclimate records of Antarctic ice-cores.
- To quantify local and regional short-term changes in surface water reservoir ages of sediment sections along the eastern and western continental margins of the southern South Pacific.
- In particular, to use these ages to uncover the differential evolution of stratification and overturning as well as the admixture of old subsurface waters along the Chilean continental margin in comparison to features observed off New Zealand.
- To better define the timing of past changes in zonal ocean circulation along the Antarctic Circumpolar Current (ACC) that may help to constrain shifts in the position of the mid-latitude Westerly belt off Chile.
- To reconstruct past local changes such as the advection of coastal waters and sea ice from Chilean fjords linked to past advances and retreats of the peak glacial Patagonian ice-sheet and a peak-glacial incursion of Antarctic icebergs in front of southern New Zealand.
- To derive the accurate pacing that controlled the outgassing or uptake of carbon in the Southern Ocean. This target demands a centennial-scale accuracy in age control.

Regional Setting

Two of our sediment records are located in the SW Pacific off Southern New Zealand, at the northern margin of the Bounty Trough (PS75-104) and, further offshore, near the mouth of this trough (SO213-76). Both sites are located in Subantarctic surface waters (Fig. 1) within the northern ACC. East of Southern New Zealand, Subantarctic surface waters impinge on a near-shore narrow tongue of salty subtropical waters advected from the north, a major conversion named Subtropical Front (STF) that forms the northern boundary of the Southern Ocean (Bostock et al., 2013). To the north the flow path of the Subantarctic inflow is topography-locked by the Chatham Rise, a ridge in the south separated from the Campbell Plateau by the deep Bounty Trough (Heath et al., 1981; Crundwell et al., 2008). Below 2000 m depth a strong Deep Western Boundary Current (DWBC) moves a volume of ~20 Sv branching off from deep parts of the ACC, a current that forms the source of Antarctic deep waters entering the West Pacific (Schmitz, 1995). During the last glacial, the patterns of surface water hydrography were shifted northward but blocked by the Chatham Rise (e.g., Bostock et al., 2013).

The hydrography along the continental margin of South Chile is influenced by ACC surface waters. Their northern branch of the ACC approaches the Chilean coast at 40°–50°S (Fig. 1), where it bifurcates into a northern branch, the Peru-Chile-Current (PCC), and a southern branch, the Cape Horn Current (CHC) (Strub et al. 1998, Chaigneau and Pizarro, 2005). Core sites MD07-3088 and PS97-137 document past changes in PCC and CHC surface waters, respectively (Fig. 1). Deep-water currents include southward flowing Pacific Deep Water (PDW) sandwiched between northward flowing

Antarctic Intermediate Waters (AAIW, 400–1200 m) and Antarctic deep and bottom waters below 3000 m (Reid, 1973; Tsuchiya and Talley, 1998).

During the last glacial, the southern Andean hinterland of both core sites was largely covered by the Patagonian Ice Sheet extending from 56°S up to 38°S and reaching the coastline south of 43°S with glaciers that formed deep fjords along the Chilean coast (Glasser and Jansson, 2008). Close to the Pacific margin of the Patagonian Ice Sheet, melt waters, rivers, and the outflow from fjords probably formed a fresh-water lid on the proximal surface ocean and delivered some ice-rafted debris (IRD) (Caniupan et al., 2011). Though there is a general consensus on ocean changes largely following an "Antarctic timing" along the Chilean margin (e.g., Lamy et al., 2007 and 2015, Caniupan et al., 2011, Haddam et al., 2018), on sub-millennial scales, the details of last glacial-to-deglacial changes in Pacific near-shore hydrography off Chile still remain somewhat uncertain. This is mainly related to a lack of robust ^{14}C reservoir ages constraining both an accurate radiocarbon-based chronology and short-term but distinctive changes in surface water ventilation.

At the Chile continental margin, local records of IRD and SST suggest a glacial advance of ice transport that culminated near the end of the LGM, 19–18 cal. ka, and during the Antarctic Cold Reversal (ACR) near 14–13 cal. ka (Caniupan et al., 2011; Darvill et al., 2016). Ice advances then were probably tied to both a northward shift of the west wind belt and enlarged melt water lids and seasonal spreading of sea ice near Chile that resulted in more stratified surface waters of the easternmost subpolar Pacific (Kohlfeld et al., 2013, Lamy et al., 2015).

Material and Methods

Our study is based on four hemipelagic sediment cores from the South Pacific (Table 1, Fig. 1). As required by the ^{14}C plateau tuning method (Sarnthein et al., 2007; Balmer and Sarnthein, 2017) the cores show on average high sedimentation rates of >10, in part >100 cm/kyr (Fig. 2a-d). These high rates are needed to compare centennial-scale ^{14}C records of planktic foraminifera with plateau structures of coeval atmospheric ^{14}C concentrations measured on plant macrofossils of the Lake Suigetsu section (Bronk Ramsay et al., 2012). In this way we deduce changes in planktic ^{14}C reservoir age (or 'reservoir effect' *sensu* Alves et al., 2018, or Marine Reservoir Age, MRA) for peak glacial and deglacial times. Occasional tephra layers independently dated nearby on land provide additional evidence in support of the age control deduced by ^{14}C plateau tuning.

Sediment samples were freeze dried, washed over a 63 µm sieve, and finally cleaned with deionized water. Monospecific planktic foraminifera tests of *Globigerinoides bulloides* (250–315 µm) and/or *Cibicidoides wuellerstorfi* (150–400 µm) were picked for stable-oxygen isotopes ($\delta^{18}O$). In Core PS75-104-1 an initial stratigraphic assessment was established by a record of X-Ray fluorescence (XRF) -based Calcium counts (AVAATECH core scanner, AWI). Stable oxygen and carbon isotopes were analyzed on 6–12 clean specimens of *G. bulloides* each with a *Finnigan MAT 253* mass spectrometer equipped with a *Kiel IV Carbonate Device*. On the basis of the initial age model we selected *G. bulloides* samples for accelerator mass spectrometry (AMS) ^{14}C analyses. In the first part of our project, 3-7 mg graphitized carbonate samples of cores PS75-104-1 and SO213-76 were analyzed at the Keck Laboratory of the University of

California Irvine. Subsequently, for each sample, we analyzed CO_2 gas of 0.6–1 mg carbonate at the Mini Carbon Dating System (MICADAS) facility of the AWI. Our data are complemented by a planktic $\delta^{18}O$ record and ^{14}C ages of ~30 *G. bulloides* samples of Core MD07-3088, that were taken from Siani et al. (2013) and Haddam et al. (2018).

Age Control Based on ^{14}C Plateau Tuning Technique

Atmospheric ^{14}C jumps and plateau boundaries in the ^{14}C record of Lake Suigetsu (SG) provide a suite of >25 age tie points between 10 and 27 cal. ka to correlate local and global changes in paleoceanography to variations in global climate (Sarnthein et al., 2007; 2015). For age control we employ the modeled $SG06_{2012}$ time scale of Bronk Ramsey et al., (2012). This scale is based on a correlation of Hulu Cave U/Th ages and has turned out as best reproducible basis for age calibrations, superior to microscopy-based varve counts (Sarnthein et al., 2020 accepted). The uncertainty of U/Th model-based age estimates rises from ~±20 at 10 cal. ka, ~±65 yr at 26 cal ka, to to ±95 yr at 29 cal ca. The error of atmospheric plateau boundary ages (half the age distance between two neighbor ages in the Suigetsu record) reaches a maximum of 140/2 = ±70 cal. yr. Sediment ages between upper and lower plateau boundaries are derived by means of linear interpolation.

A suite of ^{14}C ages is named "^{14}C plateau" if these ages form a scatter band with almost constant values, where the overall gradient is significantly lower than one ^{14}C year per calendar year, either based on visual inspection and/or on statistical evaluation by means of the first derivative of all downcore changes in the ^{14}C age – calendar age relationship (Sarnthein et al., 2015). Apart from up to 10% outliers (located outside the scatter bands of ^{14}C ages framed as plateau 'boxes') ^{14}C plateaus show an age variance of less than ±100 to ±300 ^{14}C years and extend over more than 300 years in the Suigetsu atmospheric ^{14}C record and equivalent sediment sections of planktic ^{14}C records. Prior to 25 cal. ka, the variance is reaching up to 500 ^{14}C years.

To obtain a rough initial stratigraphic guideline for splicing the succession of planktic ^{14}C plateaus to pertinent plateaus in the Suigetsu atmospheric reference record, we use planktic and/or benthic oxygen isotope ($\delta^{18}O$) records, at Site PS75-104 a record of X-ray fluorescence (XRF)-based Ca counts (a record of biogenic $CaCO_3$ content) to identify age-calibrated intervals such as the ACR, the early deglacial and LGM. In case of uncertainties in plateau assignment, the planktic ^{14}C reservoir ages derived from plateau tuning are kept as low as possible (Sarnthein et al., 2007).

In Core MD07-3088 we use tephra layers equivalents which have been ^{14}C dated on land, as independent age markers (Siani et al., 2013; Haddam et al., 2018). The same applies to a tephra layer in Core SO213-76 east of Southern New Zealand (Ronge et al., 2016).

The basic assumption of the ^{14}C plateau tuning technique is that the fine structure of fluctuations of the global atmospheric ^{14}C concentration record can also be found in the surface ocean. Here we refer to the origin and interpretation of planktic ^{14}C plateaus, assuming a global atmospheric origin with local atmospheric and oceanographic forcings. The series of planktic ^{14}C plateaus and jumps and their plateau-specific structures in a (hemipelagic) sediment age-depth record form a well-defined suite for which absolute age and reservoir age are derived by means of a strict alignment to the reference suite of global atmospheric ^{14}C plateaus as a whole. Initially, age tie points of the stable-isotope records serve as stratigraphic guideline for the alignment. Planktic reservoir ages and their short-term changes are derived from the difference in (average) ^{14}C age between atmosphere and surface waters in subsequent plateaus.

To avoid arbitrariness and to stay close to modern estimates for low latitude waters (Sarnthein et al., 2007) reservoir ages are kept at a minimum unless paired stringent evidence (e.g., paired benthic ^{14}C ages) requires otherwise. A close correspondence between ^{14}C concentrations in atmosphere and surface ocean is expected based on rapid gas exchange. In several cases, however, deviations of the specific length and structure of a planktic ^{14}C plateau from those of the pertinent atmospheric plateau within the suite of atmospheric plateaus indicate temporary local intra-plateau changes of reservoir age. Such changes may result from local changes in ocean atmosphere exchange and in oceanic mixing. As a rule, the use of the suite of plateaus in this case still provides valuable information because major millennial-scale changes in reservoir age, induced by climate change, are more widely spaced than the length of most individual ^{14}C plateaus (400-1100 yr; Sarnthein et al., 2020), which keeps plateaus recognizable. Abrupt changes in gas exchange or ocean mixing usually affect one or only a few plateaus of the suite. Absolute age estimates within a plateau are derived by linear interpolation between the age of the base and top of an undisturbed plateau assuming linear sedimentation rates. The potential impact of short-term sedimentation pulses on the formation of ^{14}C plateaus has largely been discarded by Balmer and Sarnthein (2016).

As indicated above, uncertainties in the age control of plateau boundaries are generally lower than 70 cal. yr (details in Sarnthein et al., 2020, based on Bronk Ramsey et al., 2012). Uncertainties in planktic ^{14}C reservoir ages are calculated by Gaussian error propagation including the uncertainties of calibrated age of each ^{14}C plateau at Suigetsu plus that of the coeval planktic ^{14}C plateau as well as the measurement error of each planktic ^{14}C date (Table 2).

As a valuable byproduct the high-resolution planktic ^{14}C records help to detect millennial-scale hiatuses in marine sediment records generally missed by conventional stratigraphic techniques but revealed as far more frequent than commonly assumed.

Results

Core PS75-104-1 (upper continental slope off Southern New Zealand)

Küssner et al. (2018) gave a detailed account of the top 120-long cm of sediment and ^{14}C records of Core PS75-104-1. The records are now extended down to 220 cm depth (Fig. 2a; Suppl. Table S2). XRF-based Ca counts and (raw) ^{14}C ages show carbonate-rich Holocene sediments from 0 to 25 cm. Below, decreasing carbonate contents mark the deglacial section down to 85 cm depth on top of carbonate-poor peak glacial sediments that reach down to ~250 cm depth.

Based on visual inspection we can separate two populations of planktic ^{14}C ages: Age population (1) consists of a suite of eight narrow plateau-shaped scatter bands of the maximum ^{14}C ages found in each sediment section (blue dots in Fig. 2a), plateaus that can be tuned to Suigetsu atmospheric plateaus number 1 to 4 and 6a to 8. Altogether the ^{14}C plateau boundaries result in 14 age tie points that encompass a time span of about 14.1 to 24.3 cal. ka (Table 2a). Also, they include a minor hiatus near 19.6–21 cal. ka, where we assume a loss of Plateaus 5a and b to avoid potential reservoir ages higher than 2000 years (Suppl. Table S1). This definition follows the rule always to derive the lowest-possible reservoir age (Sarnthein et al., 2007); in this case, we choose double plateau 6a and 6b instead of subsequent plateaus 5a and 5b. – The boundary between ^{14}C plateaus 6b and 7 is poorly defined because of ^{14}C ages biased by downcore burrowing activity outlined below.

Age population (2) consists of a cone-shaped array of 'aberrant' ^{14}C ages that extend from ~30 down to 180 cm core depth (red dots in Fig. 2a) and reflect the burrowing activity of *Zoophycos* (Küssner et al., 2018). The slight rise of these ages shows a gradually increasing incorporation of older foraminifera tests from the ambient host sediment. The age offset between younger foraminifera tests in the burrows and those picked from the adjacent host sediment (i.e., ^{14}C age population no. 1) varies from 900 yr near the top up to ~6000 ^{14}C yr in deeper parts of the burrow.

Different from Küssner et al. (2018), who used Suigetsu microscopy-based varve counts to derive cal. ages, the age tie points now are calibrated to U/Th model-based ages that have been transferred from the Hulu Cave record to the Suigetsu record by Bronk Ramsey et al. (2012; reasons for the revision detailed in Sarnthein et al., 2020). Resulting sedimentation rates vary from >10–35 cm/kyr during the LGM and 16–19 cm/kyr during the late deglacial, but drop to ~3 cm/kyr during the latest deglacial and Holocene. A minimum in sediment deposition also applies to the section between Plateau 2b and 3. Prior to 23 cal. ka, a lack of pertinent planktic ^{14}C data prevents us from defining the lower boundary of Plateau 8 and accurate sedimentation rates.

Surface water reservoir ages equivalent to the difference between the average ^{14}C ages of associated planktic and atmospheric ^{14}C plateaus, vary between 1650 and 1030 ^{14}C yr during peak glacial times, near 1100 yr at early deglacial plateaus 2a–3, and amount to ~800 yr at Plateau 1. After 14 cal. ka, the raw gradient of ^{14}C ages suggests that they probably drop significantly (Figs. 2a and 3).

Core SO213-76-2 (Bounty Trough east of New Zealand)

The benthic $\delta^{18}O$ record of Site SO213-76 reflects a 230 cm thick section of Holocene and deglacial sediments. Below they pass into glacial sediments reaching down to 600 cm and farther below (Fig. 2b). Off New Zealand modern benthic ^{14}C and $\delta^{18}O$ signals of deep waters at 4340 m may be delayed because of global meridional overturning circulation on average by 600–1000 ^{14}C yr (Matsumoto, 2007) in comparison to signals linked to atmospheric age tie points of surface waters that record past changes in climate and global ice volume in the North Atlantic. At 4340 m depth, the benthic $\delta^{18}O$ signal reflects signals linked to Antarctic Bottom Water (AABW) formation (McCave et al., 2008) coeval with climate changes in the Weddell Sea. Vazquez-Riveiros et al. (2010) suggest that the $\delta^{18}O$ record of benthic foraminifera in AABW lags a paired planktic record by 1.9 kyr. Accordingly, we ascribe the early deglacial ^{14}C plateau at 105–226 cm to Plateau 2b the base of which puts the onset of a deglacial benthic $\delta^{18}O$ shift to ~16.8 cal. ka.

Below Plateau 2b, the ^{14}C record shows an abrupt jump by 2000 yr, most likely the result of a hiatus on top of a brief ^{14}C plateau, possibly a fragment of Plateau 4 although no sediment structure pertinent for a hiatus was found yet near 230 cm depth. Farther below, a two-step rise in ^{14}C age leads to two major planktic ^{14}C plateaus at ~287 – 400 and 400 – 600 cm core depth, tentatively tuned to plateaus 5a and 5b (Fig. 2b, Table 2b, Suppl. Table S2). In theory, the LGM core section below the 230-cm hiatus may be assigned to alternative suites of ^{14}C plateaus, in particular, the fragment of Plateau 4. Here plateau tuning is hampered due to a general lack of initial age tie points that might provide a stratigraphic guideline for plateau assignment. The tuning mode we propose in Fig. 2b, however, leads to a suite of ^{14}C plateaus that closely resemble various details of the Suigetsu record and imply lowest-possible marine reservoir ages larger than 300 yr, moreover, long-term fairly constant sedimentation rates.

Below Plateau 5b, a hiatus spans about 3000 ^{14}C yr reaching back to the top of a poorly identified plateau structure tentatively assigned to Plateau 10a. The sediment thickness for Plateau 5a includes a major, up to 10 cm thick graded turbidite layer (also revealed by a groove mark at its base) as well as several minor turbidites that mainly consist of volcanic ash. Both their chemistry and ^{14}C ages of foraminifera grains picked from inside the graded turbidite layer suggest the Kawakawa Ash as potential origin (Ronge et al., 2016). Problems of age correlation, however, are discussed below.

Prior to ~20 cal. ka, LGM planktic reservoir ages reach 1460 yr. Later, they drop to 990 and 700 ^{14}C yr. Age-calibrated plateau boundaries suggest hemipelagic sedimentation rates of ~217–284 cm/kyr. The hiatuses below Plateau 2b and below Plateau 5b may result from erosive turbidity currents frequently runníng along the Bounty Trough (Bostock et al., 2013).

Core PS97-137-1 (upper continental margin of South Chile)

Holocene sediments in core PS97-137-1 extend from 0–50 cm with planktic $\delta^{18}O$ values of 2.0–2.5 ‰. From 50–150 cm the values increase from 2.5 to 4 ‰, which reflects the last deglacial. Below, peak glacial $\delta^{18}O$ values strongly fluctuate, possibly salinity (e.g., melt water) -induced, from 3.5 to 4.2 ‰ (Fig. 2c). Overall the $\delta^{18}O$-based stratigraphy is consistent with our high-resolution suite of planktic ^{14}C ages that extend from 2690 yr BP near to the core top back to 24,160 ^{14}C yr BP at 830 cm depth (Suppl. Table S3).

Glacial-to-deglacial ^{14}C values display a suite of nine ^{14}C plateaus, most of them with structures resembling those of Suigetsu plateaus 2a and b, 3, 4, 5a, 6a and b, 7, and 8, altogether covering a time span from 15.3 to 24.25 cal. ka (Table 2c). A pronounced ^{14}C jump of 1840 yr occurs within laminated sediments of the section between base of Plateau 4 and top of Plateau 6a, at 273 to ~320 cm depth. Our mode of plateau tuning ascribes the jump to a section with close-to-zero deposition. Here sedimentation rates drop from plateaus 3 and 4 back to 5a from 85 to 50 and 21 cm/kyr. The brief minimum culminates in a minor hiatus right at the base of Plateau 5a (disconformity displayed by distorted sediment laminations near 300 cm; Fig. S1), where up to 15 cm sediment may be lost, while Plateau 5b is hardly developed.

Instead of a quasi-hiatus near 300 cm one may assume an alternative mode of tuning with a short-term drop in local reservoir ages by 1360 yr from 2180 yr for a plateau here named '5a' (instead of '6a' in Fig. 2c) down to 1790 yr for the lowermost part of Plateau 4, here split off as plateau splinter named '4b' instead of '5a', and to 820 yr for the main portion of Plateau 4 (Fig. S2). As compared to the former tuning mode, however, this second mode leads to far more pronounced, hence less likely short-term jumps in both reservoir age and sedimentation rate (between 100 and 180 cm/kyr), thus is discarded.

Below plateau 8 (in tuning mode one; Fig. 2c) the ^{14}C record extends back to a plateau that we tuned to atmospheric Plateau 10a, ~25.9–27.0 cal. ka, when assuming a reservoir age of 900 yr per analogy to LGM reservoir ages obtained further up-core. Between a short core section below the base of Plateau 8 and a short section on top of Plateau 10a, our ^{14}C plateau tuning suggests a hiatus of ~1000 cal. yr near 680 cm core depth (Table S3; Fig. 2c). Indeed, this gap is confirmed by an erosional sediment structure depicted in Fig. 4.

On top of Plateau 4, the reservoir age of Plateau 3 shows a brief rise to 1500 ^{14}C yr at 18.2–17.5 cal. ka, that is at the vey end of the LGM. Subsequently, reservoir ages continuously decrease to ~460 ^{14}C yr at 15.4 cal. ka (Fig. 3). Based on the cal. age of ^{14}C plateau boundaries of PS97-137-1 (Suppl. Table 3; Fig. 2c), LGM sedimentation rates vary from 35–130 cm/kyr. During early deglacial plateaus 3 to 2a they drop from ~85 to ~25 cm/kyr. High sedimentation rates may be linked to increased terrigenous input from the southern Andes including pronounced pulses of sediment supply at ~23–21 and 18.2–16.5 cal. ka, then possibly linked to Patagonian ice-sheet dynamics. Accordingly, sediments below 700 cm (>25 cal. ka) contain rare pieces of IRD (Fig. S1), confirming a record of Caniupan et al. (2011).

Core MD07-3088 (Upper continental margin of southern Central Chile)

Previously published ^{14}C ages (Suppl Table S4), various chronostratigraphic proxy records (e.g., planktic foraminiferal $\delta^{18}O$, alkenone-based SSTs), and four pre-Holocene ash layers (^{14}C-dated on land) indicate that sediments in core MD07-3088 cover the last ~22 cal. kyr (Siani et al., 2010, 2013, Haddam et al., 2018; Martinez-Fontaine et al., 2019). Our newly compiled ^{14}C record based on 68 ^{14}C ages defines a suite of 11 ^{14}C plateaus from ~11 back to 22 cal. ka between 600 and 1900 cm core depth. Their internal plateau structures closely match those of the Suigetsu atmospheric ^{14}C record (Table 2d, Fig. 2d). This tuning mode is largely superior to alternative modes that try to slightly regroup the definition of plateau boundaries for plateau 4, 5a and 5b.

Different from Core PS97-137-1, ^{14}C plateaus 4 to 6a in Core MD07-3088 suggest fairly low reservoir ages of ~400 (380–450) ^{14}C yr for LGM surface waters between ~22 and 18.6 cal ka. About 1000 yr prior to the deglacial onset of rapid Antarctic warming, surface water reservoir ages started to increase to 800 and up to 1310 ^{14}C yr near the end of HS-1. During the ACR (14.35–12.8 cal. ka; Morgan et al., 2002; Buizert et al., 2015), however, surface water reservoir ages briefly dropped back to 730–940 ^{14}C yr, a clear reversal of the overall deglacial rise. This short-term drop by 600 years resulted in a (presumed) bisection of Plateau 1 (‘1 base’ and ‘1 top’). Parallel to the upper Younger Dryas (YD) reservoir ages reached a further maximum of 1750 ^{14}C yr, that lasted until 11.8 cal. ka. With the onset of the Holocene, reservoir ages dropped back to 800–950 ^{14}C yr, values that were similar to those during the ACR and the onset of HS-1. Moreover, they match reservoir ages of ~500–1100 yr recorded by Early

Holocene shells from the coastal upwelling region off Southern Peru (Fontugne et al., 2004).

Most important, the reservoir ages derived from the tuning of ^{14}C plateaus Top YD, 1a, 1, and 2b closely confirm the four reservoir ages that were deduced from the difference between ^{14}C ages of planktic foraminifera and those of paired tephra layers independently ^{14}C dated on land by the atmospheric ^{14}C age of terrestrial plants (Siani et al. 2013; Haddam et al., 2018) (Figs. 2d and 3). The highly resolved deglacial suite of planktic ^{14}C plateaus allows to further constrain the variability of marine reservoir ages between the tephra layers.

Based on the cal. age of ^{14}C plateau boundaries peak glacial sedimentation rates in core MD07- 3088 reached 140–215 cm/kyr, with a brief maximum of 730 cm/kyr between 13.5 and 16 m core depth, equivalent to 20±0.25 cal. ka (Fig. 2d; Suppl. Table S4). This sediment layer is marked by a prolonged Ti/K maximum showing that the extreme sediment supply was due to terrigenous sediment input that mainly consisted of fine sand <125 µm and silt, slightly graded near to the base of the layer (Siani et al., 2013; Suppl. Fig. 4). This grain size spectrum is characteristic of 'glacial milk', a facies suggesting nearby discharge of glacial meltwaters from the Patagonian Ice Sheet. The extreme sediment input led to a dilution of foraminiferal tests in glacial sediment samples and in turn, to a reduced temporal resolution of ^{14}C samples between 1200 and 1900 cm core depth. This results in a less precise definition of ^{14}C plateau boundaries. After 17.6 cal. ka, deglacial sedimentation rates dropped to 35-50 cm/kyr during the time equivalent of HS-1 and YD. Finally, they rose back to 120 cm/kyr right at the onset of the Holocene.

DISCUSSION

Advanced age control

Plateau boundaries in planktic ^{14}C records of four sediment cores from the southern South Pacific were tuned to pertinent atmospheric ^{14}C plateau boundaries to provide a new level in the accuracy of centennial-to-millennial-scale age control and the global age correlation of South Pacific paleoceanographic records to terrestrial records including ice-cores.

A unique characteristic of our sediment records is the occasional occurrence of tephra that have been independently dated on land. Previous studies used tephra chronologies to improve the knowledge of glacial-to-deglacial reservoir ages (Sikes et al., 2000; Rose et al., 2010; Siani et al., 2013; Skinner et al., 2015; Sikes and Guilderson, 2016; Shao et al., 2019; Stott et al., 2019; Martinez-Fontaine et al., 2019). In particular, the authors used ^{14}C ages of marine carbonates deposited below and/or on top of rare volcanic tephra layers erupted over the last 30 kyr. Reservoir ages of these carbonates were deduced from the difference obtained for (atmospheric) ^{14}C ages of organic material of land-based deposits paired with the same tephra. In comparison to the ^{14}C plateau tuning, the irregular occurrence of tephra layers, unfortunately, does not provide the high density of narrow-spaced tie points. Off Chile, our calibrated ^{14}C ages closely correspond to ages previously derived from four tephra over the last deglaciation. Off New Zealand, however, our plateau tuning suggests a depositional age different from that previously assigned.

Several authors (Carter et al., 1995; Rose et al., 2010; Sikes et al., 2016) used the Late Pleistocene Kawakawa ash layer, erupted from New Zealand, as tie point for ages in SW Pacific sediment cores. The terrestrial ^{14}C age of Kawakawa ash amounts to 22.59 ±0.23 ka equal to 26.3 cal. ka, later revised to 25.36 cal. ka (Carter et al., 1995; Vandergoes et al., 2013; Lowe et al., 2013). In Core SO213-76-2, however, ^{14}C plateau tuning revealed for the ~10 cm thick layer of Kawakawa ash a depositional age of ~18,5 ^{14}C yr equal to ~20 cal. ka, 5000 yr less than previously suggested. Both a groove mark near the base and clear sediment gradation show that the ash layer was likely dispersed by a major turbidite current followed by several small turbidites shortly thereafter (Fig. 2b). Planktic foraminifera picked near the base of the turbidite layer showed an age of 21.9 ^{14}C ka. This value indeed comes closer to the terrestrial ^{14}C age estimate if we assume a low, though unknown marine reservoir age of ~200 yr for the source region of the displaced foraminiferal tests. In summary, our ^{14}C plateau-based cal. ages show that the occurrence of a Kawakawa ash layer in sediments of the Bounty Trough off New Zealand *per se* may not always be appropriate as age tie point, since the ash may have been dispersed by subsequent turbidites up to >5000 yr after the eruption. The ^{14}C age of foraminifers reworked near the base of the turbidite indeed comes close to the actual age of Kawakawa ash originally proposed.

For the LGM, the quality of ^{14}C plateau-based age control was corroborated by evidence independently obtained from Subantarctic Site PS97-137 off South Chile. High-resolution core photography of the Plateau-8 sediment section (500–643 cm core depth; 22.94–24.25 cal. ka; Figs. 2c and 4b) reveals continuous fine-scale lamination. Similar laminae mark most of LGM Plateaus 4 to 6a, moreover, sediments assigned to Plateau 10a. On average, one cm of laminated sediment contains about eight to twelve layers, which implies some 960–1440 layers for the ~140 cm long sediment section of Plateau 8. This number comes close to ~1300 years, the interval contained in atmospheric Plateau 8, hence suggesting annual layering and giving independent support for the age range deduced by ^{14}C plateau tuning.

We surmise that the laminae resulted from seasonal variations in glaciomarine sediment deposition, despite a lack of organic-carbon enrichment that is widely characteristic of oxygen minimum zones and sediment lamination. By contrast, the layers formed in a basically oxic environment. Possibly nutrient supply was that low that it precluded any bottom life needed for bioturbational mixing. Also, the laminated sediments contain some ice-rafted debris. The laminated facies may be similar to one reported by Stein (2008) for late deglacial sediments off East Greenland, deposited during glacier retreat and/or seasonal sea-ice cover, moreover, to that of contourite ridges in the LGM Weddell Sea possibly deposited below coastal polynyas (Sprenk et al., 2014).

Implications for deglacial changes in South Pacific surface water hydrology

Based on Parennin et al. (2013), Marcott et al. (2014), and the WDC record (Sigl et al., 2016) the last deglaciation started in West Antarctica with a 4000 yr long period of slow, millennial-scale mode warming near 21.8 cal. ka. In contrast, abrupt, centennial-scale warming of West *and* East Antarctica only started at 17.6±0.1 cal. ka (Fig. 3). As postulated by the bipolar seesaw concept (Stocker and Johnson, 2003), this date is coeval with the onset of Heinrich Stadial 1 (HS1) in the northern Hemisphere. Also, it matches the onset of the deglacial rise in atmospheric pCO_2 (Fig. 3a/b) and, in particular, the top of atmospheric ^{14}C Plateau 3 at 17.5 cal. ka (Fig. 2) within an uncertainty range of ~±50 yr (Sarnthein et al., 2020).

Based on this global age tie point we can now directly correlate the onset of rapid Antarctic warming to the very top of the LGM maximum in planktic $\delta^{18}O$, thus constrain the precise age of the beginning of major $\delta^{18}O$ decrease in our two sediment records off Chile (Figs. 2c,d). However, the onset of a prominent SST rise (Uk37 and foraminifera assemblages; Haddam et al., 2018), that is the onset of local deglacial warming, lags the paired $\delta^{18}O$ signal by ~100-200 yr at Site MD07-3088 (Fig. 2d) .The lead of enhanced planktic $\delta^{18}O$ depletion may thus primarily reflect an early incursion of meltwaters. This conclusion would be in line with an abrupt shift in the composition of terrigenous sediment input at MD07-3088 (Fig. S4; Siani et al., 2013). Moreover, it parallels the onset of deglacial Patagonian ice sheet retreat between 17.77 and 17.38 cal. ka (Bendle et al., 2019).

Transferring our ^{14}C plateau-based chronology of Core PS75-104-1 (for the interval ~14-24 cal. ka) to neighbor Core MD97-2120 (using XRF data; Fig. S3) results in cal. ages for MD97-2120 about 1500 yr younger than those proposed by Pahnke et al. (2003 a, b). This correlation shifts the onset of deglacial warming in the Uk37-based SST record of Core MD97-2120 (Pahnke and Sachs, 2006) (Figs. 3c and S3) from 19.1 to 17.6 cal. ka, that is, precisely coeval with the beginning of fast deglacial warming in Antarctic ice-cores.

In addition to the initiation of rapid warming in Antarctica coeval with Heinrich event cooling in the northern hemisphere, the timing of short-term interhemispheric climate oscillations later during the last deglaciation (i.e., Antarctic Cold Reversal (ACR)) provide a test case for the bipolar seesaw (Stocker and Johnsen, 2003). In harmony with the ages reported from Antarctic ice cores (Buizert et al., 2015, the planktic $\delta^{18}O$ record of Core MD07-3088 off Central Chile (Fig. 2d) indeed reflects an ^{18}O enrichment during the ACR that terminated near 12.8 cal. ka, that is, right after the base of a ^{14}C plateau named 'YD' (12.9 cal. ka). The paired Uk37-based SST record (Siani et al., 2013) suggests a brief cooling that preceded the $\delta^{18}O$ signal by few 100 years and ended with a first minor warming already as early as 13.7 cal. ka, thus implies that changes in sea surface salinity were a major driver of variations in $\delta^{18}O$ during the ACR.

Planktic reservoir ages as tracer of surface water history

Beyond high-resolution age control, ^{14}C plateau tuning provides novel details on the spatio-temporal variation of planktic Marine Reservoir Ages (MRA) over last glacial-to-deglacial times. This claim was validated by four tephra-based reservoir ages in Core MD07-3088 that closely match our robust MRA estimates based on ^{14}C plateau tuning (Fig. 2d and 3). As outlined in the introduction, past MRA are regarded as robust tracer of the origin and fate of local surface waters along the South Pacific margins and are compared to coeval shifts in atmospheric pCO_2 and its stable carbon isotope ($\delta^{13}C$) composition (Fig. 3).

In general, low MRA (<500 yr) suggest extensive surface water ventilation and unimpeded uptake of atmospheric CO_2 such as off southern Central Chile (MD07-3088 at 46°S), where – different from previous assumptions (Martinez-Fontaine et al., 2019) – ages of ~400 yr continued over the LGM, 22–18.5 cal. ka. We thus may infer open-sea conditions, minimum surface water stratification, possibly linked to local convection ~~which, however, contradicts the supposed glacial setting~~ close to the Patagonian Ice

Sheet (Davies et al., 2020). Vivid LGM mixing of surface waters at Site MD07-3088 was coeval with major shifts in benthic $\Delta^{14}C$ that record coeval changes in Antarctic Intermediate Water formation (Haddam et al., 2020; Siani et al., 2013; Martinez-Fontaine et al., 2019).

Off Southern Chile (PS97-137 at ~53°S) brief changes in ^{14}C reservoir age during the late LGM and early deglacial may also be linked to short-term changes in coastal outline and/or regional Patagonian ice sheet geometry and dynamics during this time (Figs. 1, 3b). These changes involved periods of reduced or enhanced melt water input that induced changes in offshore surface water stratification and ventilation. Peak glacial surface waters off Southern Chile show MRA of 600–1200, finally reaching 1500 yr (Fig. 3). These values are in harmony with a paleoenvironmental setting close to the Pacific margin of the glacial Patagonian ice sheet (Caniupan et al. (2011).

Only after the onset of rapid Antarctic warming, 17.5 cal. ka, MRA started to drop to 450 yr, at site PS97-137. Likewise, a striking brief low in local MRA occurred over Plateau 8 (equivalent to HS-2 / GIS 2). The low may be linked to a transient coeval warming in Antarctica, a trend corresponding to the MAR drop during HS-1 (Fig. 3). Off southernmost Chile both events may probably reflect brief time spans with open-sea conditions and enhanced admixture of atmospheric CO_2 possibly linked to a brief latitudinal shift of the Subantarctic Front in response to Heinrich Events.

Last glacial MRAs at both Chilean sites, only 800 km apart from each other, differ by 400-800 yr (Fig. 3b). During the last deglaciation, MRA at northern Site MD07-3088 started to rise, while MRAs decreased towards values of 400 yr further south. The opposed trends might be explained by an LGM advection of upwelled waters from the Polar Frontal Zone not reaching the northern site where surface water ventilation remained high.

In the Southwest Pacific, high glacial MRA values of 1000–1650 yr were recorded both at sites PS75-104 and SO213-076-2 (Fig. 3a). Here peak glacial surface waters were poorly ventilated probably due to predominant stratification, a hydrographic setting controlled by icebergs and local meltwaters immediately east, that is leeward of glaciated Southern New Zealand. This regime is documented by ice-rafted debris along the northern fringe of the LGM Antarctic Circumpolar Current then advanced far north (Bostock et al., 2013; Carter et al, 2002). The stratification hindered a free exchange of atmospheric CO_2 over several thousand years (*sensu* Sessford et al., 2019, in the Nordic Seas), a regime that continued over early deglacial times until ~15 cal. ka. Off New Zealand it also extended farther east, up to Bounty Trough Site SO213-76 (Fig. 3), where MRA also reach values of 1500-1000 yr, though IRD is largely absent from this region (Bostock et al., 2013). At this site the stratification may have merely resulted from a far eastward extension of New Zealand borne melt water and stratification. Alternatively, high MRA values may also result from an upwelling of old subsurface waters from below that also entails, however, an enhanced productivity of local surface waters (Sarnthein et al., 2015, 2019; Balmer and Sarnthein, 2018). We hardly find any traces of high productivity near to our Southwest Pacific sites.

With regard to sediment cores east of New Zealand, most authors used the global and/or marine calibration curves IntCal13 for age control (Reimer et al., 2013), now to be replaced by IntCal20 (Reimer et al., 2020). Sikes and Guilderson (2016) assumed that surface reservoir ages during the late deglaciation and early Holocene did not differ much from the recent value of 400 ±100 yr. Their glacial-to-early-deglacial reservoir ages of subtropical surface waters ranged from ~600 to 700 yr, compared to much higher values of 3200 yr estimated for Subantarctic waters. Shao et al. (2019), in turn, converted the planktic ^{14}C ages of a Chatham Rise core to calendar years by means of the BChron Bayesian chronology package (Haslett & Parnell, 2008). This technique requires previous knowledge of surface water reservoir ages, derived from, e.g., the ^{14}C age of the Kawakawa ash (Lowe et al., 2013), which implies a glacial-to-early deglacial reservoir age of ~1600–1300 yr. These values differ little from 1000–1200 yr inferred by Skinner (2015; Fig .5) and in particular, from 1000–1650 yr derived by ^{14}C plateau tuning for Core PS75-104-1 offshore Southern New Zealand, an island then strongly glaciated and located south of the influence of subtropical waters (Bostock et al., 2013; Fig. 1, 2a, 3c).

Our estimates of glacial-to-deglacial MRAs were compared to an overview of MRAs compiled by Skinner et al. (2019) on the basis of various age tie points and IntCal13 for cores from the Southern Ocean (Fig. 5). By its trend, however, the spline curve of Skinner et al. does not reflect but envelopes the array of our estimates. In particular, it does not display the ongoing extreme spatio-temporal variability of MRA, which underlines the need to establish detailed region-specific MAR records (Fig. 3a and b) for ^{14}C dating purposes.

CONCLUSIONS

– Robust centennial-scale age control was established for last glacial and deglacial sediment sections in four marine sediment cores to obtain a detailed and precise stratigraphic correlation between both the western and eastern continental margins of the southern South Pacific and paleoclimate records of Antarctic ice cores.

– Off central Chile four tephra layers provide independent proof for precise age assignment and marine reservoir ages derived by means of the ^{14}C plateau technique. Inversely, the Kawakawa ash layer in the Bounty Trough off New Zealand entails a more complex view on tephra-based age assignment: ^{14}C plateau tuning and sediment structures indicate that the tephra was supplied by a turbidity current that spread only 5,000 yr after volcanic ash eruption. The age of ash formation, however, is partially recorded in the tephra layer by the ^{14}C age of foraminifera tests reworked near the base of the turbidite.

– Our ^{14}C plateau-based age control suggests that the onset of fast West Antarctic warming dated in ice cores near 17.6 cal. ka is also reflected by a robust tipping point in planktic $\delta^{18}O$ records from the eastern South Pacific. This date is coeval with the onset of Heinrich Stadial 1 within the range of age uncertainty, hence confirms the concept of bipolar seesaw. Likewise, the plateau-tuning technique shows that the end of the ACR in a core off southern central Chile was precisely coeval with the onset of the YD cold spell in the northern Hemisphere.

–Our revised stratigraphy suggests that the local onset of Uk37-based deglacial warming off New Zealand was synchronous with the onset of the main temperature rise in Antarctica at 17.6 cal. ka.

– East of Southern New Zealand, along the Bounty Trough, glacial MRA reach 1000-1500 yr here probably recording widespread surface water stratification linked to icebergs and meltwater also documented by ice-rafted debris. This regime continued until ~15.5 cal. ka.

– During the LGM, surface waters off southern Chile (46°S) are marked by low planktic ^{14}C reservoir ages of ~400 yr. Low MRA reflect a maximum exchange of carbon with the atmosphere, indicative of open sea conditions and overturning surface waters.

– By contrast, high MRA off Chile at 53°S range from 900–1200 yr that may largely reflect a local stratification of surface waters by melt waters of icebergs, in part documented by ice-rafted debris. Moreover, high MRA may be linked to northward advection of upwelled old subsurface waters from the Polar Frontal Zone.

– High MRAs off southern Chile are linked to sediments that show fine-scale laminations, and partly IRD. Assuming a process of annual sediment layering, the number of laminae largely confirms the age control inferred from ^{14}C plateau boundaries. The laminations possibly reflect a depositional environment covered by meltwaters similar to that of the Greenland Sea and near the Filchner-Rønne Ice Shelf.

Acknowledgments

We acknowledge M. Mudelsee, Bad Gandersheim, for calculating the 1st derivative and 1-σ uncertainty range of our planktic ^{14}C records. We thank R. Stein (AWI) for valuable discussions on laminated polar sediments and P.M. Grootes (University of Kiel) for helpful comments, K. Pahnke for providing XRF data, M. Seebeck, L. Schönborn, E. Bonk, H. Grotheer, and T. Gentz (AWI) for technical support. We acknowledge J. Southon (University of California Irvine, CA) for measuring numerous ^{14}C ages of cores PS75-104-1 and SO213-76-2, and the funding through the AWI Helmholtz-Zentrum für Polar- und Meeresforschung internal strategy fund (COPTER project) for long-term support. All ^{14}C values are listed in Suppl. Table S1 - S4. Mass spectrometric and ^{14}C data are stored at www.PANGAEA.de (PDI-24801).

REFERENCES

Alves, E. Q., Macario, K., Ascough, P., Bronk Ramsey, C. (2018). The worldwide marine radiocarbon reservoir effect: Definitions, mechanisms, and prospects. *Reviews of Geophysics*, 56. https://doi.org/10.1002/2017RG000588

Balmer, S., & Sarnthein, M. (2017). Planktic ^{14}C plateaus: A result of short-term sedimentation pulses? Radiocarbon, *59*(1), 33-43. DOI:10.1017/RDC.2016.100

Balmer, S., & Sarnthein, M. (2018). Glacial-to-deglacial changes in North Atlantic meltwater advection and deep-water formation – Centennial-to-millennial-scale ^{14}C records from the Azores Plateau. *Geochimica et Cosmochimica Acta*, 236. https://doi.org/10.1016/j.gca.2018.03.001

Balmer, S., Sarnthein, M., Mudelsee, M., Grootes, P. M. (2016). Refined modeling and ^{14}C plateau tuning reveal consistent patterns of glacial and deglacial ^{14}C reservoir ages of surface waters in low-latitude Atlantic. *Paleoceanography and Paleoclimatology*, 31. https://doi.org/10.1002/2016PA002953

Bauska, T. K., Brook, E. J., Marcott, S. A., Baggenstos, D., Shackleton, S., Severinghaus, J. P. & Petrenko, V. V. (2018). Controls on millennial-scale atmospheric CO_2 variability during the last glacial period. *Geophysical Research Letters*, 45, 7731–7740. https://doi.org/10.1029/2018GL077881

Bendle, J., Palmer, A., Thorndycraft, V., Matthews, I. (2019). Phased Patagonian Ice Sheet response to Southern Hemisphere atmospheric and oceanic warming between 18 and 17 ka. *Scientific Reports*, 9, 4133. https://doi.org/10.1038/s41598-019-39750-w

Benz, V., Esper, O., Gersonde, R., Lamy, F., Tiedemann, R. (2016). Last Glacial Maximum sea surface temperature and sea-ice extent in the Pacific sector of the Southern Ocean. *Quaternary Science Reviews*, 146, 216–237. https://doi.org/10.1016/j.quascirev.2016.06.006

Bostock, H. C., Sutton, P. J., Williams, M. J. M., Opdyke, B. N. (2013). Reviewing the circulation and mixing of Antarctic Intermediate Water in the South Pacific using evidence from geochemical tracers and Argo float trajectories. *Deep Sea Research Part 1: Oceanographic Research Papers*, 73, 84–98. https://doi.org/10.1016/j.dsr.2012.11.007

Bronk Ramsey, C., Staff, R. A., Bryant, C. L., Brock, F., Kitagawa, H., van der Plicht, J., et al. (2012). A complete terrestrial radiocarbon record for 11.2 to 52.8 kyr BP. *Science*, 338 (6105), 370–374. https://doi.org/10.1126/science.1226660

Buizert, C., Adrian, B., Ahn, J. et al. (2015). Precise interpolar phasing of abrupt climate change during the last ice age. *Nature* 520**,** 661-665. https://doi.org/10.1038/nature14401

Buizert, C., Sigl, M., Severi, M., Markle, B. R., Wettstein, J. J., McConnell, J. R. et al. (2018). Abrupt ice-age shifts in southern westerly winds and Antarctic climate forced from the north. *Nature* 563**,** 681-685. https://doi.org/10.1038/s41586-018-0727-5

Caniupán, M., Lamy, F., Lange, C. B., Kaiser, J., Arz, H., Kilian, R., et al. (2011). Millennial-scale sea surface temperature and Patagonian Ice Sheet changes off southernmost Chile (53°S) over the past similar to 60 kyr. *Paleoceanography and Paleoclimatology*, 26, PA3221. https://doi.org/10.1029/2010PA002049

Carter, L., Manighetti, B., Ganssen, G., Northcote, L. (2008). Southwest Pacific modulation of abrupt climate change during the Antarctic Cold Reversal–Younger Dryas. *Palaeogeography, Palaeoclimatology, Palaeoecology*, 260, 284-298. https://doi.org/10.1016/j.palaeo.2007.08.013

Carter, L., Neil, H., Northcote, L. (2002). Late Quaternary ice-rafting events in the SW Pacific Ocean, off eastern New Zealand. *Marine Geology*, 191. 19-35. https://doi.org/10.1016/S0025-3227(02)00509-1

Carter, L., Nelson, C. S., Neil, H. L., Froggatt, P. C. (1995). Correlation, dispersal, and preservation of the Kawakawa Tephra and other late Quaternary tephra layers in the Southwest Pacific Ocean. *New Zealand Journal of Geology and Geophysics*, 38:1, 29-46. https://doi.org/10.1080/00288306.1995.9514637

Chaigneau, A. & Pizarro, O. (2005). Surface circulation and fronts of the South Pacific Ocean, east of 120°W. *Geophysical Research Letters*, 32. https://doi.org/10.1029/2004GL022070

Crundwell, M., Scott, G., Naish, T., Carter, L. (2008). Glacial–interglacial ocean climate variability from planktonic foraminifera during the Mid-Pleistocene transition in the temperate Southwest

Pacific, ODP Site 1123. *Palaeogeography, Palaeoclimatology, Palaeoecology*, 260, 202-229. https://doi.org/10.1016/j.palaeo.2007.08.023

Darvill, C. M., Bentley, M. J., Stokes, C. R., Shulmeister, J. (2016). The timing and cause of glacial advances in the southern mid-latitudes during the last glacial cycle based on a synthesis of exposure ages from Patagonia and New Zealand. *Quaternary Science Reviews*, 149, 200– 214. https://doi.org/10.1016/j.quascirev.2016.07.024

Denton, G. H., Anderson, R. F., Toggweiler, J. R., Edwards, R. L., Schaefer, J. M., Putnam, A. E. (2010). The Last Glacial Termination. *Science*, 328, 1652-1656. https://doi.org/ 10.1126/science.1184119

De Pol-Holz, R., Keigwin, L. D., Southon, J., Hebbeln, D., Mohtadi, M. (2010). No signature of abyssal carbon in intermediate waters off Chile during deglaciation. *Nature Geoscience*, 3, 192–195. https://doi.org/10.1038/ngeo745

Fontugne, M., Carré, M., Bentleb, I., Julien, M., Lavallée, D. (2004). Radiocarbon reservoir age variations in the South Peruvian upwelling during the Holocene. *Radiocarbon*, 46 (2), 531-537.

Glasser, N., & Jansson, K. (2008). The glacial map of southern South America. *Journal of Maps*, 4(1), 175–196. https://doi.org/10.4113/jom.2008.1020

Haddam, N., Siani, G., Michel, E., Kaiser, J., Lamy, F., Duchamp-Alphonse, S., et al. (2018). Changes in latitudinal sea surface temperature gradients along the Southern Chilean margin since the last glacial. *Quaternary Science Reviews*, 194. https://doi.org/10.1016/j.quascirev.2018.06.023

Haslett, J., & Parnell, A. (2008). A Simple Monotone Process with Application to Radiocarbon-Dated Depth Chronologies. *Journal of the Royal Statistical Society Series C (Applied Statistics)*, 57, 399–418. https://doi.org/10.1111/j.1467-9876.2008.00623.x

Heath, R. A (1981). **Physical oceanography of the waters over the Chatham Rise.** New Zealand Oceanographic Institute, Oceanography Summary, 18, pp. 15.

Kawamura, K., Parrenin, F., Lisiecki, L. et al. (2007). Northern Hemisphere forcing of climatic cycles in Antarctica over the past 360,000 years. *Nature*, 448, 912–916. https://doi.org/10.1038/nature06015

Khatiwala, S., Schmittner, A., Muglia, J. (2019). Air-sea disequilibrium enhances ocean Carbon storage during glacial periods. *Science Advances*, 5, no. 6. https://doi.org/10.1126/sciadv.aaw4981

Kohfeld, K. E., Graham, R., De Boer, A., Sime, L. C., Wolff, E. W., Le Quéré, C., & Bopp, L. (2013): Southern Hemisphere westerly wind changes during the Last Glacial Maximum: Paleo-data synthesis. *Quaternary Science Reviews*, 68, 76–95. https://doi.org/ 10.1016/j.quascirev.2013.01.017

Küssner, K., Sarnthein, M., Lamy, F., Tiedemann, R. (2018). High-resolution radiocarbon records trace episodes of *Zoophycos* burrowing. *Marine Geology*, 403, 48-56. https://doi.org/10.1016/j.margeo.2018.04.013

Lamy, F., Arz, H. W., Kilian, R., Lange, C. B., Lembke-Jene, L., Wengler, et al. (2015). Glacial reduction and millennial-scale variations in Drake Passage throughflow. *Proceedings of the National Academy of Sciences*, 112(44), 13,496–13,501. https://doi.org/10.1073/pnas.1509203112

Lamy, F., Chiang, J. C. H., Martínez-Méndez, G., Thierens, M., Arz, H. W., Bosmans, J., et al. (2019). Precession modulation of the South Pacific westerly wind belt over the past million years. *Proceedings of the National Academy of Sciences*, 116, no. 47, 23455-23460. https://doi.org/10.1073/pnas.1905847116

Lamy, F., Kaiser, J., Arz, H., Hebbeln, D., Ninnemann, U., Timm, O., et al. (2007). Modulation of the bipolar seesaw in the Southeast Pacific during Termination 1. *Earth and Planetary Science Letters*, 259. 400-413. https://doi.org/10.1016/j.epsl.2007.04.040

Locarnini, R. A., Mishonov, A. V., Antonov, J. I., Boyer, T. P., Garcia, H. E., Baranova, O. K., et al. (2013). World Ocean Atlas 2013, Volume 1: Temperature. Levitus, S., Ed., Mishonov. A., Technical Ed.; NOAA Atlas NESDIS 73, pp. 40.

Lourantou, A., Lavric, J. V., Köhler, P., Barnola, J.-M., Paillard, D., Michel, E., et al. (2010). Constraint of the CO_2 rise by new atmospheric carbon isotopic measurements during the last deglaciation. *Global Biogeochemical Cycles*, 24, GB2015, doi:10.1029/2009GB003545

Lowe, D., Blaauw, M., Hogg, A., Newnham, R. (2013). Ages of 24 widespread tephras erupted since 30,000 years ago in New Zealand, with re-evaluation of the timing and palaeoclimatic implications of the Late glacial cool episode recorded at Kaipo bog. *Quaternary Science Reviews*, 74, 170-194. https://doi.org/10.1016/j.quascirev.2012.11.022

Marcott, S. A., Bauska, T. K., Buizert, C., Steig, E. J., Rosen, J. L., Cuffey, K. M., et al. (2014). Centennial scale changes in the global carbon cycle during the last deglaciation. *Nature*, 514, 616–619. https://doi.org/10.1038/nature13799

Martínez Fontaine, C., De Pol-Holz, R., Michel, E., Siani, G., Reyes-Macaya, D., Martínez Méndez, G., et al. (2019). Ventilation of the deep ocean carbon reservoir during the last deglaciation: results from the southeast pacific. *Paleoceanography and Paleoclimatology*, 34 (12), 2080-2097. https://doi.org/10.1029/2019PA003613

Matsumoto, K. (2007). Radiocarbon-based circulation age of the world oceans. *Journal of Geophysical Research*, 112, C09004. https://doi.org/10.1029/2007JC004095

Marzocchi, A. & Jansen, M. F. (2019). Global cooling linked to increased glacial carbon storage via changes in Antarctic sea ice. *Nature Geoscience,* 12, 1001–1005. https://doi.org/10.1038/s41561-019-0466-8

Morgan, V., Delmotte, M., Van Ommen, T., Jouzel, J., Chappellaz, J., Woon, S., et al. (2002). Relative Timing of Deglacial Climate Events in Antarctica and Greenland. *Science*, 297, 1862-1864. https://doi.org/10.1126/science.1074257

Moy, A. D., Palmer, M. R., Howard, W. R., Bijma, J., Cooper, M. J., Calvo, E., et al. (2019). Varied contribution of the Southern Ocean to deglacial atmospheric CO_2 rise. *Nature Geoscience.* 12, 1006–1011. https://doi.org/10.1038/s41561-019-0473-9

Pahnke, K., & Zahn. R. (2005). Southern Hemisphere water mass conversion linked with North Atlantic climate variability. *Science*, 307, 1741–1746. https://doi.org/10.1126/science.1102163

Pahnke, K., Zahn, R., Elderfield, H., Schulz. M. (2003a): 340,000-year centennial-scale marine record of Southern Hemisphere climatic oscillation, *Science*, 301, 948–952. https://doi.org/10.1126/science.1084451

Pahnke, K., Zahn, R., Elderfield, H., Schulz. M. (2003b): 340,000-Year centennial-scale marine record of Southern Hemisphere climatic oscillation. Science, 301, Supplementary Material.

Parrenin, F., Masson-Delmotte, V., Köhler, P., Raynaud, D., Paillard, D., Schwander, J., et al. (2013). Synchronous Change of Atmospheric CO2 and Antarctic Temperature During the Last Deglacial Warming. *Science*, 339, 1060-1063. https://doi.org/10.1126/science.1226368

Reid, J. L. (1973). Transpacific hydrographic sections at lats. 43°S and 28°S: The SCORPIO expedition, III, Upper water and a note on southward flow at mid-depth. *Deep Sea Research and Oceanographic Abstracts*, 20, 39-49. https://doi.org/10.1016/0011-7471(73)90041-7

Reimer P.J., Bard E., Bayliss A., Beck J. W., Blackwell P. G., Bronk Ramsey C., et al. (2013). IntCal13 and Marine13 radiocarbon age calibration curves 0–50,000 years cal BP. *Radiocarbon*, 55, 1869–1887. https://doi.org/10.2458/azu_js_rc.55.16947

Reimer, P.J. et al., (2020). The IntCal 20 northern hemisphere radiocarbon calibration curve (0-55 kcal BP). Radiocarbon, (in press).

Ronge, T. A., Tiedemann, R., Lamy, F., Kohler, P., Alloway, B. V., De Pol-Holz, R., et al. (2016). Radiocarbon constraints on the extent and evolution of the South Pacific glacial carbon pool. *Nature Communications*, 7, 11487. https://doi.org/10.1038/ncomms11487

Ronge, T. A., Prange, M., Mollenhauer, G., Ellinghausen M., Kuhn, G., Tiedemann, R. (2020). Radiocarbon evidence for the contribution of the Southern Indian Ocean to the evolution of atmospheric CO_2 over the last 32,000 years. Paleoceanography and Paleoclimate, 35, e2019PA003733, https://doi.org/10.1029/2019PA003733

Rose, K., Sikes, E., Guilderson, T., Shane, P., Hill, T., et al. (2010). Upper-ocean-to-atmosphere radiocarbon offsets imply fast deglacial carbon dioxide release. *Nature*, 466, 1093-1097. https://doi.org/10.1038/nature09288

Sarnthein, M., Balmer, S., Grootes, P.M., Mudelsee, M. (2015). Planktic and benthic ^{14}C reservoir ages for three ocean basins, calibrated by a suite of ^{14}C plateaus in the glacial-to-deglacial Suigetsu atmospheric ^{14}C record. *Radiocarbon*, 57, 129–151. https://doi.org/10.2458/azu_rc.57.17916

Sarnthein, M., Grootes, P.M., Kennett, J.P., Nadeau, M.-J. (2007). ^{14}C Reservoir Ages Show Deglacial Changes in Ocean Currents and Carbon Cycle. *Washington DC American Geophysical Union Geophysical Monograph Series*, 173, 175-196. https://doi.org/10.1029/173GM13

Sarnthein, M., Küssner, K., Grootes, P. M., Ausin, B., Eglinton, T., Muglia, J., et al. (2020). Plateaus and jumps in the atmospheric radiocarbon record – Potential 1 origin and value as global age markers for glacial-to-deglacial paleoceanography, a synthesis. *Climate of the Past*. (accepted for publ.)

Sarnthein M., Schneider B., Grootes, P. M. (2013). Peak glacial ^{14}C ventilation ages suggest major draw-down of carbon into the abyssal ocean. *Climate of the Past*, 9, 925–965. https://doi.org/10.5194/cp-9-2595-2013

Schlitzer, R., Ocean Data View, odv.awi.de, 2018.

Schmitt, J., Schneider, R., Elsig, J., Leuenberger, D., Lourantou, A., Chappellaz, J., et al. (2012). Carbon Isotope Constraints on the Deglacial CO_2 Rise from Ice Cores. *Science*, 336, 711-714. https://doi.org/10.1126/science.1217161

Schmitz, W. J. (1995). On the interbasin-scale thermohaline circulation. *Reviews of Geophysics*, 33, 151-173. https://doi.org/10.1029/95RG00879

Sessford, E. G., Jensen, M. F., Tisserand, A. A., Muschitiello, F., Dokken, T., Nisancioglu, K. H., & Jansen, E. (2019). Consistent fluctuations in intermediate water temperature off the coast of Greenland and Norway during Dansgaard-Oeschger events. *Quaternary Science Reviews*, 223. https://doi.org/10.1016/j.quascirev.2019.105887

Shao, J., Stott, L., Gray, W., Greenop, R., Pecher, I., Neil, H., et al. (2019). Atmosphere-Ocean CO_2 Exchange Across the Last Deglaciation From the Boron Isotope Proxy. *Paleoceanography and Paleoclimatology*, 34. https://doi.org/10.1029/2018PA003498

Siani, G., Colin, C., Michel, E., Carel, M., Richter, T., Kissel, C., & Dewilde, F. (2010). Late Glacial to Holocene terrigenous sediment record in the Northern Patagonian margin: Paleoclimate implications. *Palaeogeography, Palaeoclimatology, Palaeoecology*, 297, 26-36. https://doi.org/10.1016/j.palaeo.2010.07.011

Siani. G., Michel, E., De Pol-Holz, R., DeVries, T., Lamy, F., Carel, M., et al. (2013). Carbon isotope records reveal precise timing of enhanced Southern Ocean upwelling during the last deglaciation. *Nature Communications*, 4, 2758. https://doi.org/10.1038/ncomms3758

Sigl, M., Fudge, T. J., Winstrup, M., Cole-Dai, J., Ferris, D., McConnell, J. R., et al. (2016). The WAIS Divide deep ice core WD2014 chronology – Part 2: Annual-layer counting (0–31 ka BP). *Climate of the Past*, 12, 769–786, https://doi.org/10.5194/cp-12-769-2016

Sigman, D. M., Hain, M. P., Haug, G. H. (2010). The polar ocean and glacial cycles in atmospheric CO_2 concentration. *Nature*, 466, 47–55. https://doi.org/10.1038/nature09149

Sikes, E. L., Cook, M., Guilderson, T. (2016). Reduced deep ocean ventilation in the Southern Pacific Ocean during the last glaciation persisted into the deglaciation. *Earth and Planetary Science Letters*, 438, 130-138. https://doi.org/10.1016/j.epsl.2015.12.039

Sikes, E. L., & Guilderson T. P. (2016). Southwest Pacific Ocean surface reservoir ages since the last glaciation: Circulation insights from multiple-core studies. *Paleoceanography and Paleoclimatology*, 31. 298–310, https://doi.org/10.1002/2015PA002855

Sikes, E. L., Samson, C. R., Guilderson, T. P., Howard. W. R. (2000). Old radiocarbon ages in the southwest Pacific Ocean during the last glacial period and deglaciation. *Nature*, 405, 555–559, https://doi.org/10.1038/35014581

Skinner, L. C., McCave, I. N., Carter, L., Fallon, S., Scrivner, A. E., & Primeau, F. (2015). Reduced ventilation and enhanced magnitude of the deep Pacific carbon pool during the last glacial period. *Earth and Planetary Science Letters*, 411, 45–52. https://doi.org/10.1016/j.epsl.2014.11.024

Skinner, L. C., Muschitiello, F., Scrivner, A. E. (2019). Marine reservoir age variability over the last deglaciation: Implications for marine carbon cycling and prospects for regional radiocarbon calibrations. *Paleoceanography and Paleoclimatology*, 34, 1807–1815. https://doi.org/10.1029/2019PA003667

Sprenk, D., Weber, M. E., Kuhn, G., Wennrich, V., Hartmann, T., Seelos, K. (2014). Seasonal changes in glacial polynya activity inferred from Weddell Sea varves. *Climate of the Past*, 10, 1239–1251. https://doi.org/10.5194/cp-10-1239-2014

Stein. R. (2008). Arctic Ocean sediments: processes, proxies, and paleoenvironment. *Elsevier*, **ISBN:** 9780444520180

Stocker, T. F., & Johnsen, S. J. (2003). A minimum thermodynamic model for the bipolar seesaw. *Paleoceanography and Paleoclimatology*, 18, 1087. https://doi.org/10.5194/cp-10-1239-201410.1029/2003PA000920

Stott, L., Davy, B., Shao, J., Coffin, R., Pecher, I., Neil, H., et al. (2019). CO_2 Release From Pockmarks on the Chatham Rise-Bounty Trough at the Glacial Termination. *Paleoceanography and Paleoclimatology*, 34. https://doi.org/10.1029/2019PA003674

Strub, P. T., Mesias, J. M., Montecino, V., Ruttlant, J., Salinas, S. (1998). Coastal ocean circulation off Western South America. *The Sea*, 11. The Global Coastal Ocean: Regional Studies and Syntheses, edited by Robinson, A. R. and Brink, K. H., pp. 273–315, Wiley, New York.

Timmermann, A., Friedrich, T., Timm, O. E., Chikamoto, M. O., Abe-Ouchi, A., Ganopolski, A. (2014). Modeling obliquity and CO_2 effects on Southern Hemisphere climate during the past 408 ka. *Journal of Climate*, 27, 1863–1875. https://doi.org/10.1175/JCLI-D-13-00311.1

Toggweiler, J. R., Russell, J. L., Carson, S. R. (2006). Midlatitude westerlies, atmospheric CO_2, and climate change during the ice ages. *Paleoceanography and Paleoclimatology*, 21. https://doi.org/10.1029/2005PA001154 PA2005

Tsuchiya, M. & Talley, L. D. (1998). Pacific hydrographic section at 88 degree W: Water-property distribution. *Journal of Geophysical Research*, 103, no. C6, 12,899-12,918. https://doi.org/10.1029/97JC03415

Vandergoes, M. J., Hogg, A. G., Lowe, D. J. L., Newnham, R. M., Denton, G. H., Southon, J., et al. (2013). A revised age for the Kawakawa/Oruanui tephra, a key marker for the Last Glacial Maximum in New Zealand. *Quaternary Science Reviews*, 74, 195-201. https://doi.org/10.1016/j.quascirev.2012.11.006P

Wilson, D.J., Struve, T., van der Flierdt, T., Chen, T., Tao, L., Burke, A., Robinson, L.F. (2020). Sea-ice control on deglacial lower cell circulation changes recorded by Drake Passage deep-sea corals. *Earth and Planetary Science Letters*, 544, 116405. https://doi.org/l0.l016/j.epsl.2020.l 16405

TABLE CAPTIONS

Table 1. Details of core locations and selection of ^{14}C samples

Sea Region	Chatham Rise (NZ)	Bounty Trough (NZ)	Chilean Margin	Chilean Margin
Core ID	PS75-104-1	SO213-76-2	MD07-3088	PS97-137-1
Latitude/Longitude	44° 46‘ S / 174° 31‘ E	46° 12‘ S / 178° 1.6‘ W	46° 04‘ S / 75° 41‘ W	52° 39.6‘ S / 75° 33.9‘ W
Water depth	835	4339	1536	1027
Sediment facies	Homogenous silt to clay	Homogenous silt to clay, smaller turbidites, one major tephra layer	Silty clay with sandy layers	Homogenous silt to clay, in part sandy, LGM: laminated (Pl. 6a), major and minor unconformities
No. of planktic ^{14}C Ages	8 + 56[a,b]	48 + 9[a]	68 + 25[c]	59
Planktic species	*G. bulloides*	*G. bulloides*	*G. bulloides*	*G. bulloides*
No. of tests/ Weight/^{14}C sample	60 - 353 (>1.1 mg)	40 - 500 (>0.9 mg)	20 - 376 (>0.9 mg)	37 - 136 (>0.5 mg)
No. of tephra layers	-	3[a]	6[c,d]	-

a) Ronge et al. (2016) b) Küssner et al. (2018) c) Siani et al. (2013) d) Haddam et al. (2018)

Table 2a-d. Definition of planktic ^{14}C plateaus in PS75-104-1, SO213-76-2, PS97-137-1, and MD07-3088 aligned to Suigetsu atmospheric ^{14}C plateaus (lower panel). Plateau boundaries defined by visual inspection, ^{14}C jumps defined maximums in the 1st derivative of the ^{14}C gradient vs. core depth (top panel).

Table 2a

Definition of planktic ^{14}C plateaus in PS75-104-1 (defined by visual inspection)

Plateau no.	Age top (cal yr)	Depth (cm)	Age base (cal yr BP)	Depth (cm)	PS75-104-1 ø^{14}C yr BP	Suigetsu Plateau Ø^{14}C yr BP	Pla. Res. Age (yr)	1 σ error (±yr)
1	14160	40	15100	57.5	13283	12471	810	280
2a	15420	59.5	16520	77	14590	13406	1180	350
2b ?	16520	77	16930	?	15040	13850	1190	?
3	17500	86	18220	109	15765	14671	1090	265
4	18650	114	19590	135	17360	15851	1500	340
Hiatus								
6a	21000	137	21890	155	18700	17667	1030	270
6b	21890	155	22300	170 ?	19350	18075	1275	285
7	22400	176 ?	22870	192	20320	18843	1480	210
8	22940	192	24250	205	21360	19715	1650	320

Table 2b

Definition of planktic ^{14}C plateaus in SO213-076-2 (defined by visual inspection)

Plateau no.	Age top (cal yr)	Depth (cm)	Age base (cal yr BP)	Depth (cm)	SO213-076-2 ø^{14}C yr	Suigetsu Plateau Ø^{14}C yr BP	Pla. Res. Age (yr)	1 σ error (yr)
2b	16520	109.5	16930	226	14693	13850	840	312
Hiatus 4	--	--	19590	270	16548	15851	700	225
5a	19720	266	20240	400	17410	16670	990	340
5b	20240	416.5	20900	600	18466	17007	1460	515
Hiatus								
10a	25880	655	?	?		22328	?	?

Table 2c

Definition of planktic ^{14}C plateaus in PS97-137-1 (defined by visual inspection)

Plateau no.	Age top (cal yr BP)	Depth (cm)	Age base (cal yr BP)	Depth (cm)	PS97-137-1 ø^{14}C yr BP	Suigetsu Plateau Ø^{14}C yr BP	Pla. Res. Age (yr)	1 σ error (yr)
2a	15420	91	16520	121	13861	13406	455	270
2b	16520	121	16930	151	14518	13850	670	90
3	17500	161.5	18220	214.5	16177	14671	1500	180
4	18650	223.5	19590	273	16670	15851	820	225
5a	19720	276	20240	292	17643	16670	970	93
Hiatus		296						
6a	21000	321.5	21890	397	18851	17667	1185	406
6b	21890	397	22300	447	19260	18075	1185	202
7	22400	455	22900	521	19730	18843	885	276
8	22900	521	24250	643	20315	19715	600	465
Hiatus		681						
10a	25880	695	27000	728	22525	22328	900	365

Table 2d
Definition of planktic ^{14}C plateaus in MD07-3088 (defined by visual inspection)

Plateau no.	Age top (cal yr BP)	Depth (cm)	Age base (cal yr BP)	Depth (cm)	MD07-3088 ø^{14}C yr BP	Suigetsu Plateau Ø^{14}C yr BP	Pla. Res. Age (yr)	1 σ Error (yr)
Preboreal	10560	?	11108	617.5	10331	9525	806	180
Top YD	11281	629	11755	685.5	11006	10060	946	195
YD	11895	694	12475	721	12121	10380	1741	160
1a	13656	744	14042	763	12948	12006	942	125
1 top	14160	764	14450 (interpol.)	782	13200	12471	729	190
1 base	14570 (interpol.)	788	15100	811	13780	12471	1309	190
2a	15420	822	16520	858	14462	13406	1060	275
2b	16520	858	16930	873	14937	13850	1087	85
3	17500	889	18220	968	15470	14671	799	125
4	18650	1070	19590	1195	16296	15851	445	230
5a	19720	1315	20240	1620.5	17104	16667	435	140
6a ?	21000	1748	21890	1870	18051	17667	384	315
Tephra Layers	**Depth (cm)**	**Terrestrial conventional ^{14}C Age**		**Cal. Age (yr BP)**		**MD07-3088 ø^{14}C yr**	**Reservoir age (yr)**	
Tephra	660.5	9960[a]		11260-11390 *		11006 (Pl. Top YD)	1050	
Tephra	750.5	11910[a]		13720-13770 *		12948 (Plateau 1a)	1040	
Tephra	800.5	12435[a]		14160-15100		13780 (Plateau 1)	1345	
Tephra	870	13650[b]		16340-16450 *		14937 (Plateau 2b)	1290	
		a) Siani et al. 2013, b) Haddam et al. 2018		*Based on Intcal13 tree rings				

FIGURE CAPTIONS

Fig. 1. Bathymetry of the eastern and western continental margins of the southern South Pacific. Red stars mark position of sediment cores. (a) Margin off New Zealand, (b) Margin off Southern Chile. Thin broken lines show modern position of ocean fronts: SAF (purple, hatched) – Sub-Antarctic Front (Bostock et al. 2013), STF (orange) – Subtropical Front (Carter et al. 2008). Blue broken lines show position of modern ocean currents (Carter et al. 2008; Siani et al. 2013): ECC – East Cape Current, EAUC – East Auckland Current, DWBC – Deep Western Boundary Current, SC – Southland Current. PCC – Peru-Chile Current, CHC – Cape Horn Current, and ACC – Antarctic Circumpolar Current. Map plotted with OceanDataView; Schlitzer, R. ODV (2018, odv.awi.de)

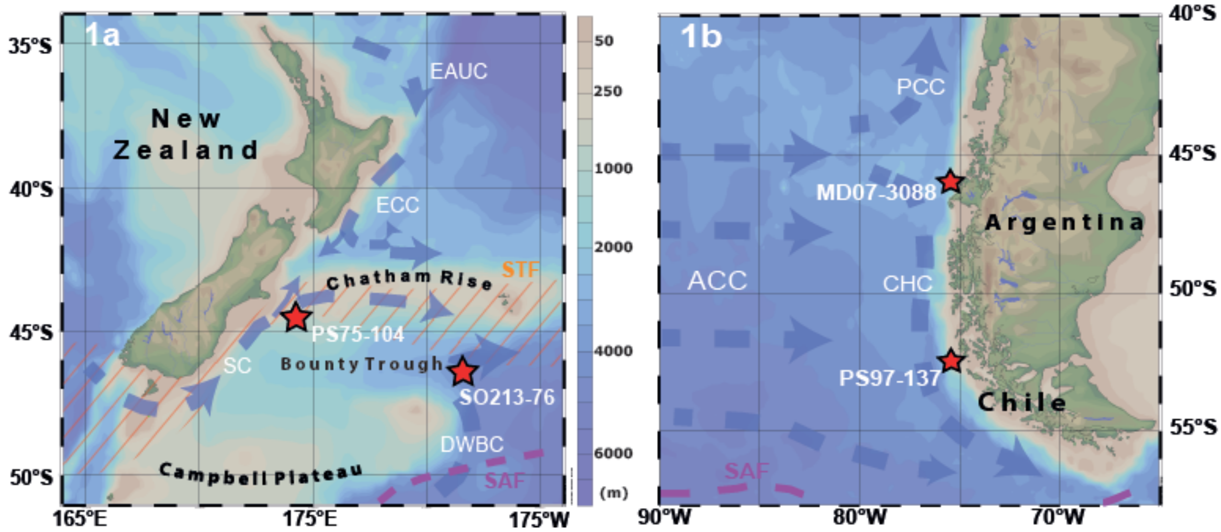

Fig. 2a-d. Planktic ^{14}C records measured on four South Pacific sediment cores (Table 1; Fig. 1; Suppl. Table S1–4) and plotted vs. core depth. Scatter bands of largely coeval planktic ^{14}C ages depict suite of planktic ^{14}C plateaus (framed by horizontal boxes) that are compared to the suite of atmospheric (atm) ^{14}C plateaus defined in the Lake Suigetsu record (^{14}C ages of Bronk Ramsey et al., 2012), where atm. ^{14}C ages are given to the left, U/Th-based calibrated (cal.) model ages below. Local planktic reservoir ages (in blue) present the difference between the average uncorrected ^{14}C age of a planktic ^{14}C plateau measured in a core and the average ^{14}C age of equivalent atm. ^{14}C plateaus numbered 1–10 (bold numbers/names in brackets). Top panels in Figs. 2a-d show units of the 1st derivative and 1-σ uncertainty range of the planktic ^{14}C record (^{14}C yr per cm core depth), with peak values indicating ^{14}C jumps (constrained by asterisks) that confine ^{14}C plateaus (numbered in black). B/A = Bølling-Allerød, HS1 and HS2 = Heinrich Stadial 1 and 2, LGM = Last Glacial Maximum, ACR = Antarctic Cold Reversal, YD = Younger Dryas. Sedimentation rates are deduced from Suigetsu-based cal. ages of plateau boundaries.

(2a) Planktic ^{14}C record and paired XRF record of Ca counts in Core PS75-104-1 (data of Küssner et al., 2018, suppl. below 120 cm core depth). Red dots reflect aberrant planktic ^{14}C ages (i.e., ages that are “too young” as compared to the suite of ^{14}C plateaus) that result from downcore reworking of foraminiferal tests in a Zoophycos burrow (Küssner et al., 2018).

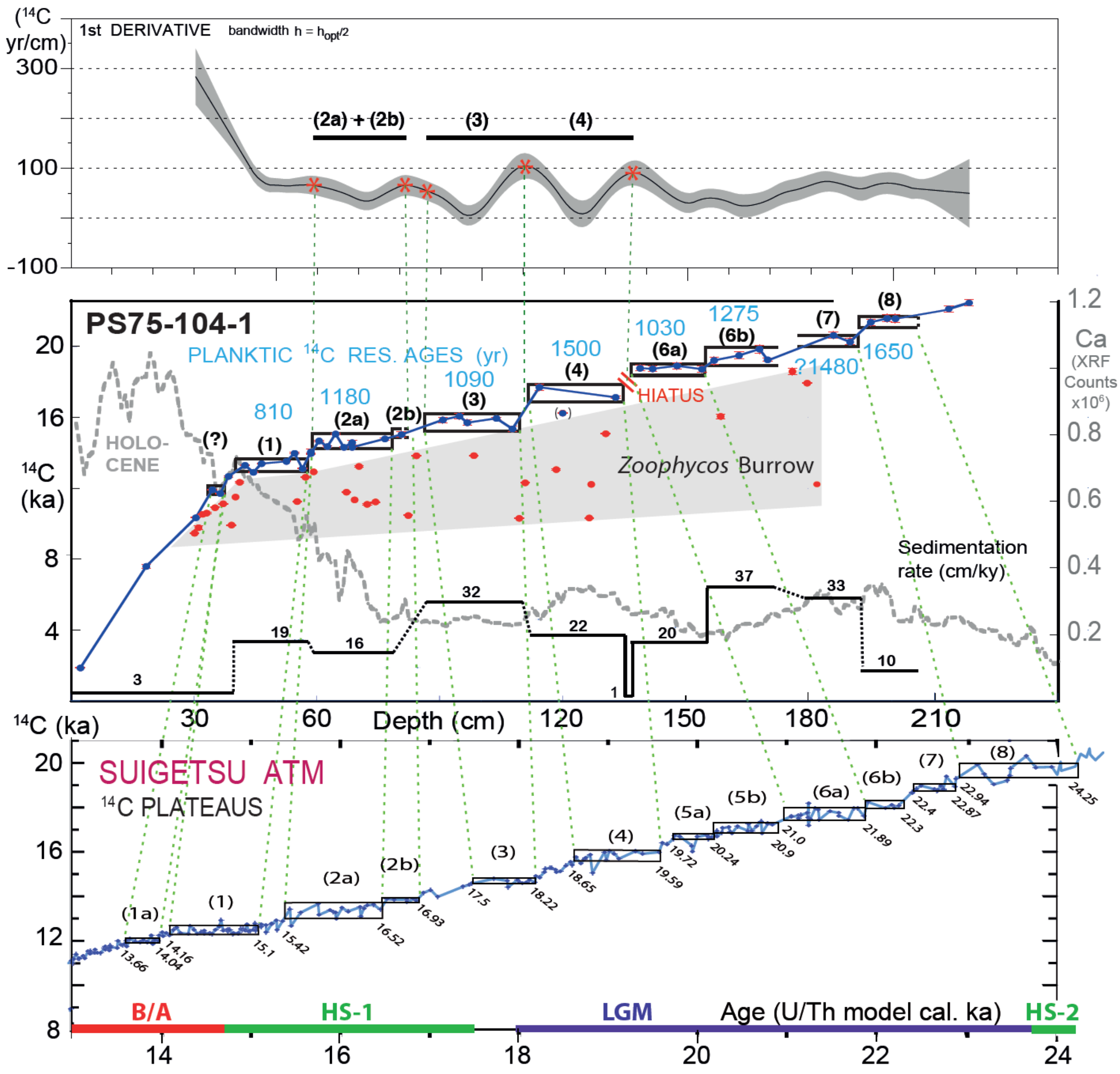

(2b) Planktic ^{14}C record and paired benthic $\delta^{18}O$ record of Core SO213-76-2. Hiatus near 238 cm assigned tentatively.

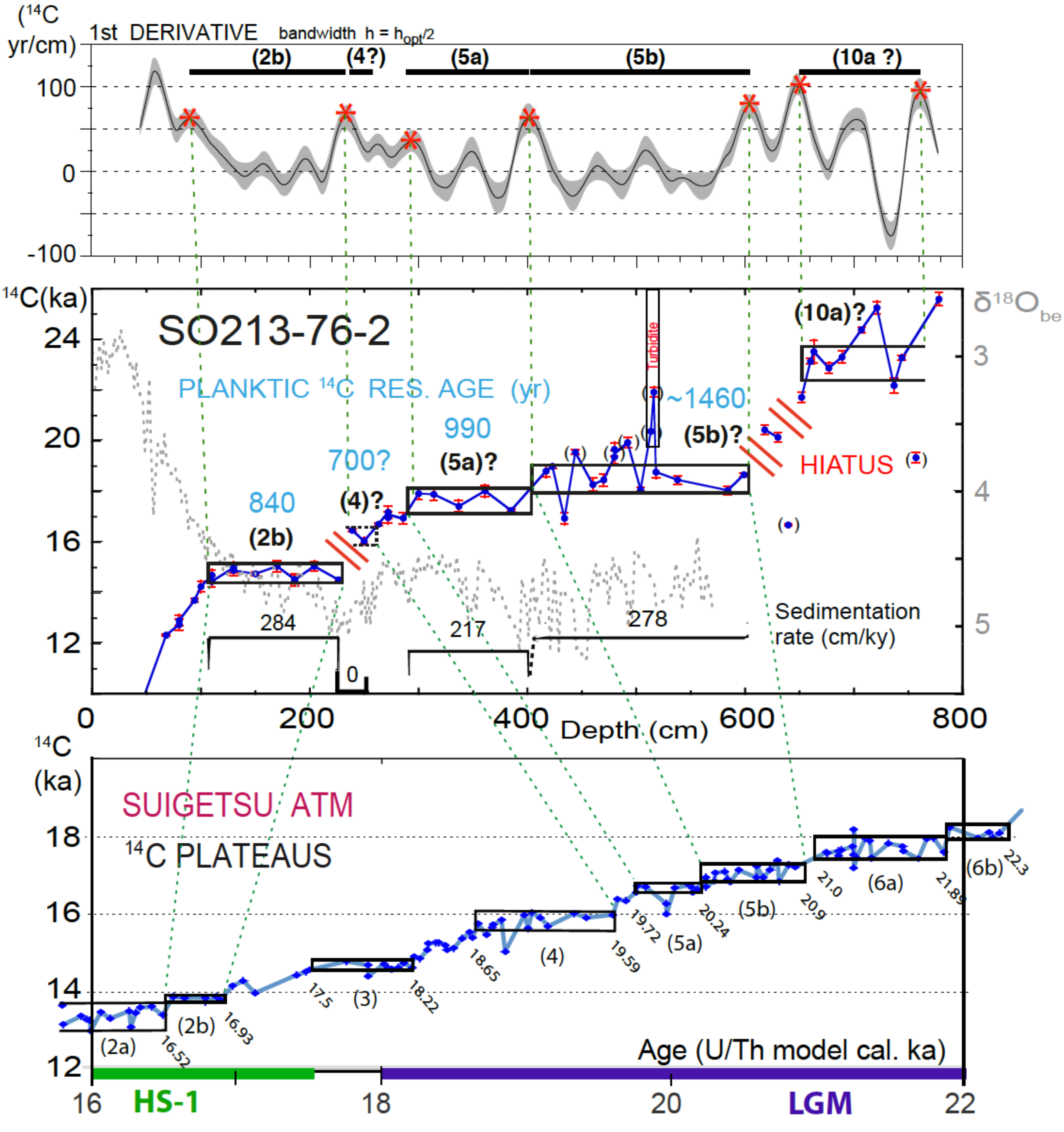

(2c) Paired planktic ^{14}C and $\delta^{18}O$ records of Core PS97-137-1. Hatched line marks sediment laminations; 'D' = Minor unconformities within the suite of laminae, 'H' = Major erosional unconformity. Sediments below 700 cm contain rare pieces of IRD.

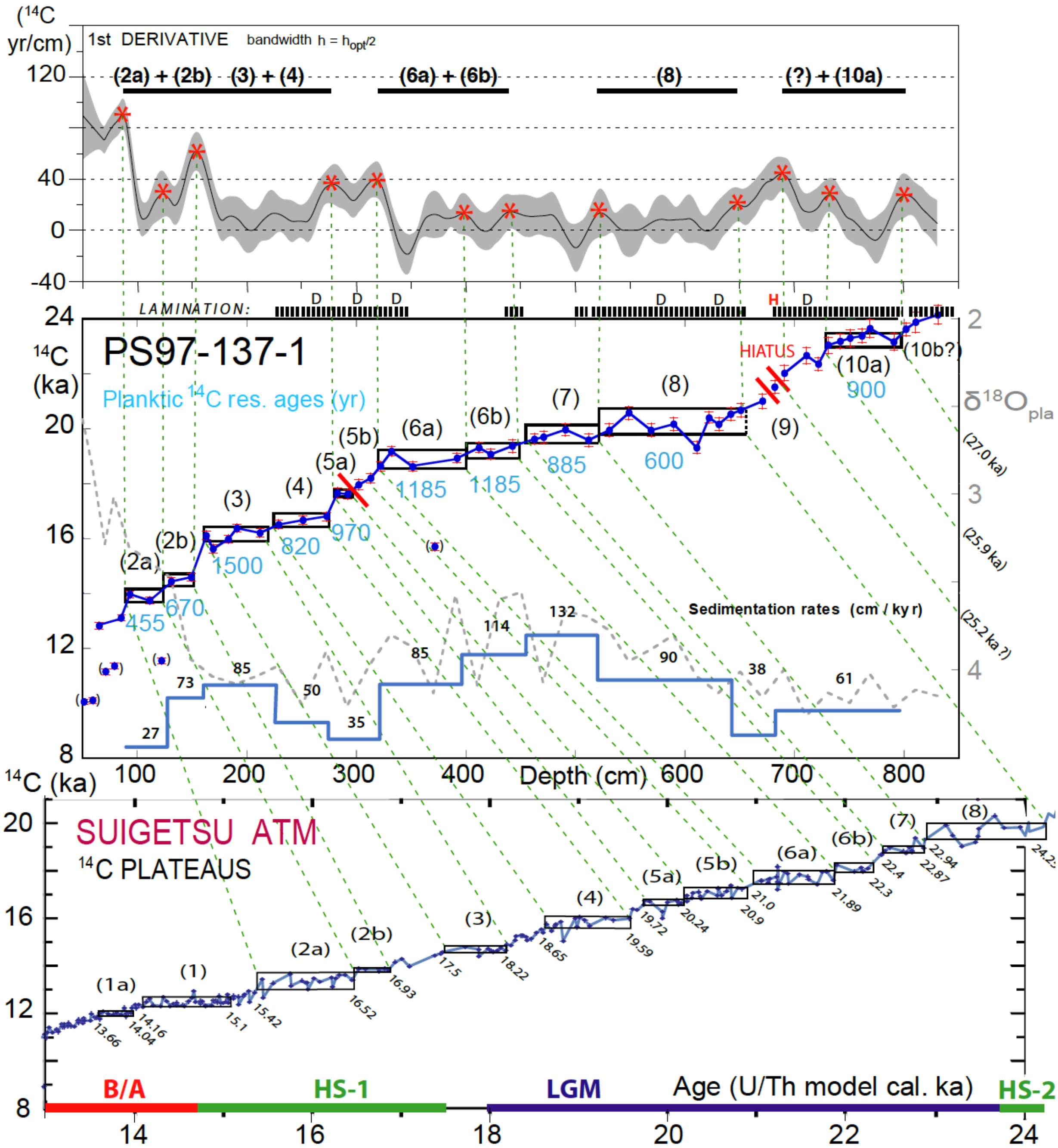

(2d) Paired planktic ^{14}C and $\delta^{18}O$ records of Core MD07-3088 (^{14}C ages of Siani et al., 2013, and this study). Bold red dots mark age position of tephra layers ^{14}C dated on land (Siani et al., 2013; Haddam et al., 2018). Plateau 5a covers graded layer of glacial fine sand and silt (Fig. S4). Below, plateau 5b assigned tentatively.

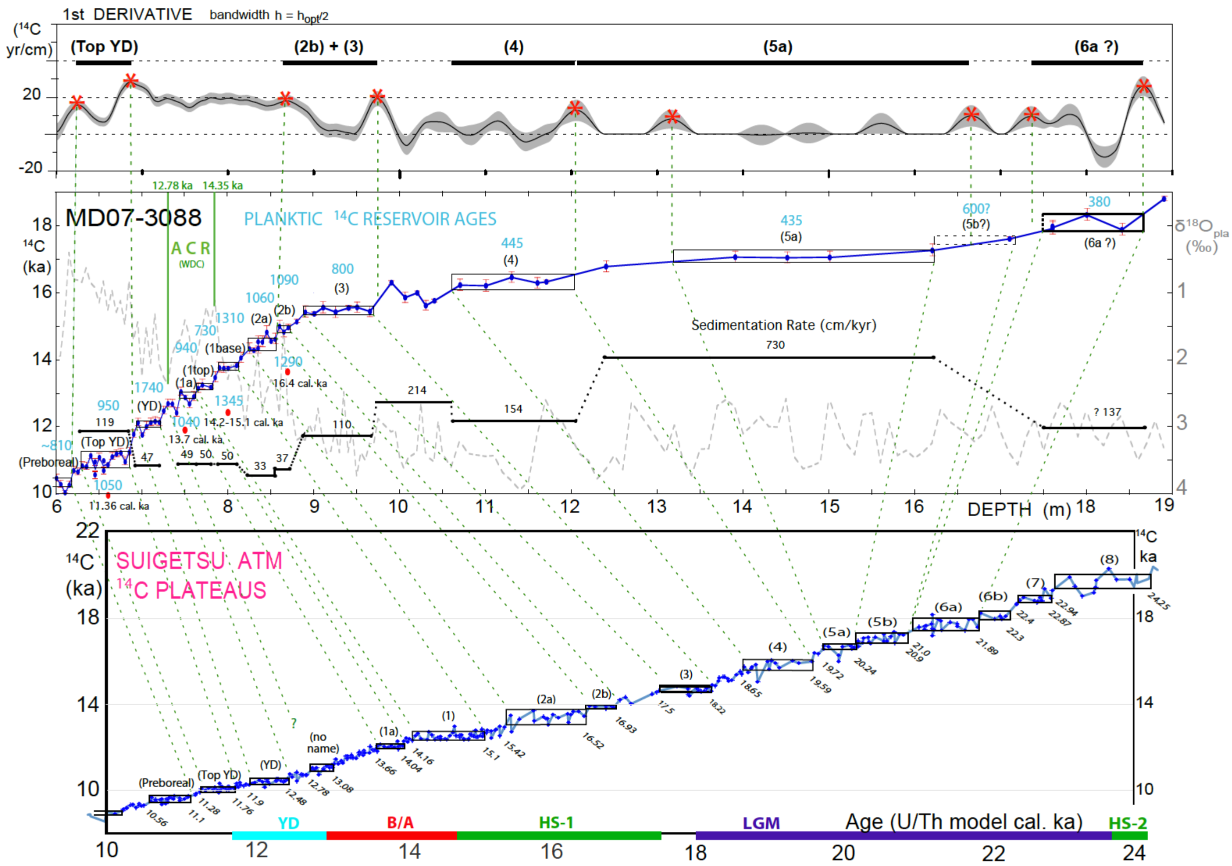

Figure 3a and b. Temporal and spatial variations in planktic (pla.) ^{14}C reservoir age recorded at sites in the western and eastern South Pacific (core locations marked in Fig. 3c). Bold red bars give paired tephra-based reservoir ages in Core MD07-3088 (Siani et al., 2013; ref.). Reservoir ages are compared to records of contemporaneous changes in West Antarctic $\delta^{18}O$ and pCO_2 (WDC Project Members, 2013; Marcott et al., 2014) and coeval changes in atm. $\delta^{13}C$ (Schmitt et al., 2012). Stratigraphic units are marked at diagram base: Younger Dryas (YD), Antarctic Cold Reversal (ACR), Bølling-Allerød (B/A), Heinrich Stadial 1 and 2 (HS-1 and HS-2), Last Glacial Maximum (LGM). Figure 3c. Modern mean annual SST (°C; Locarnini et al., 2013) in southern South Pacific and LGM extent of winter sea ice, Patagonian and New Zealand ice sheets (Darvill et al., 2016), and oceanic fronts. Red stars = core locations, white polygons off New Zealand reflect icebergs documented by ice rafted debris (Bostock et al. 2013). SAF (hatched purple shading) = Sub-Antarctic Front, STF (broken orange line) = Subtropical Front (Carter et al., 2008, Bostock et al., 2013, Benz et al., 2016; own data). Estimates of LGM Winter Sea Ice (WSI) (white lines) show maximum (>15%) and average sea-ice concentrations (40%) of winter sea-ice during September (Benz et al. 2016). Whitish shading = Area of maximum LGM vs. modern SST anomaly (Kelvin) for summer (SSST) (Benz et al. 2016).

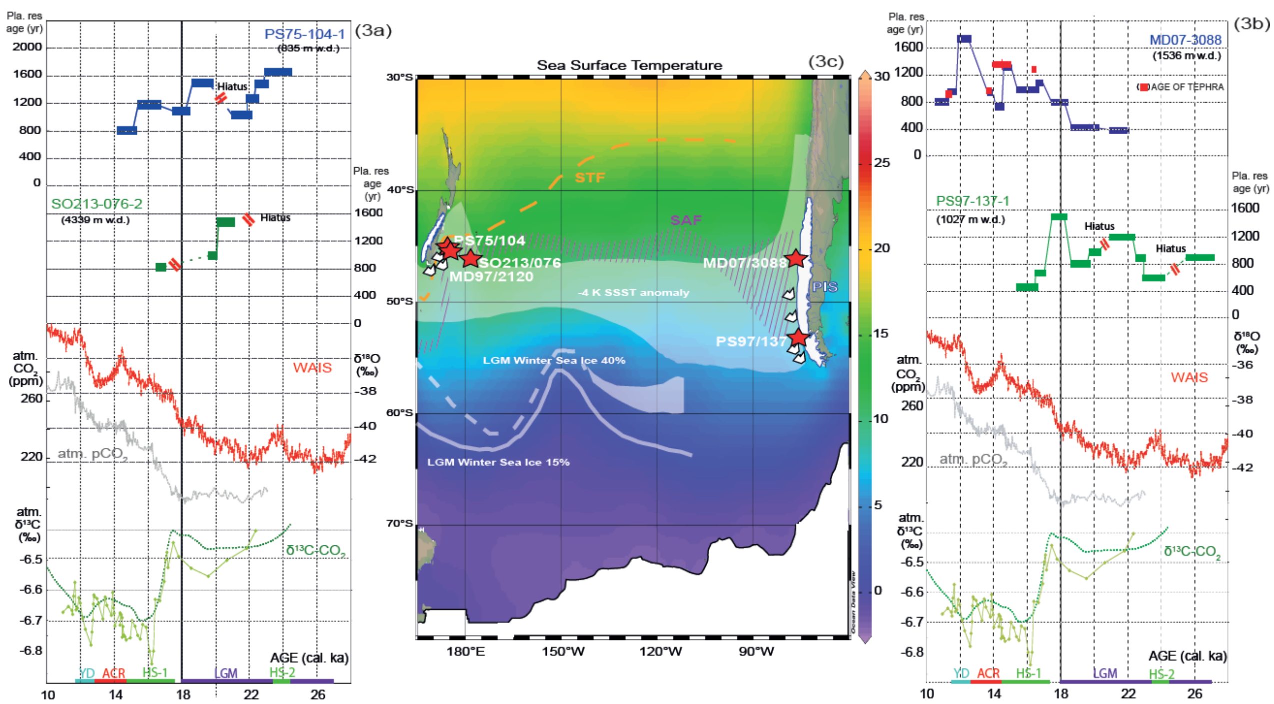

Fig. 4. Photography of sediment fabrics in Core PS97-137-1. (a) 678-686 cm and (b) 561- 572 cm depth, showing a major LGM disconformity at 681.5 cm core depth (white broken line line outlines two dark horizontal grove structures cut off at their top) and millimeter-scale laminations. Sediment photographies were slightly brightened.

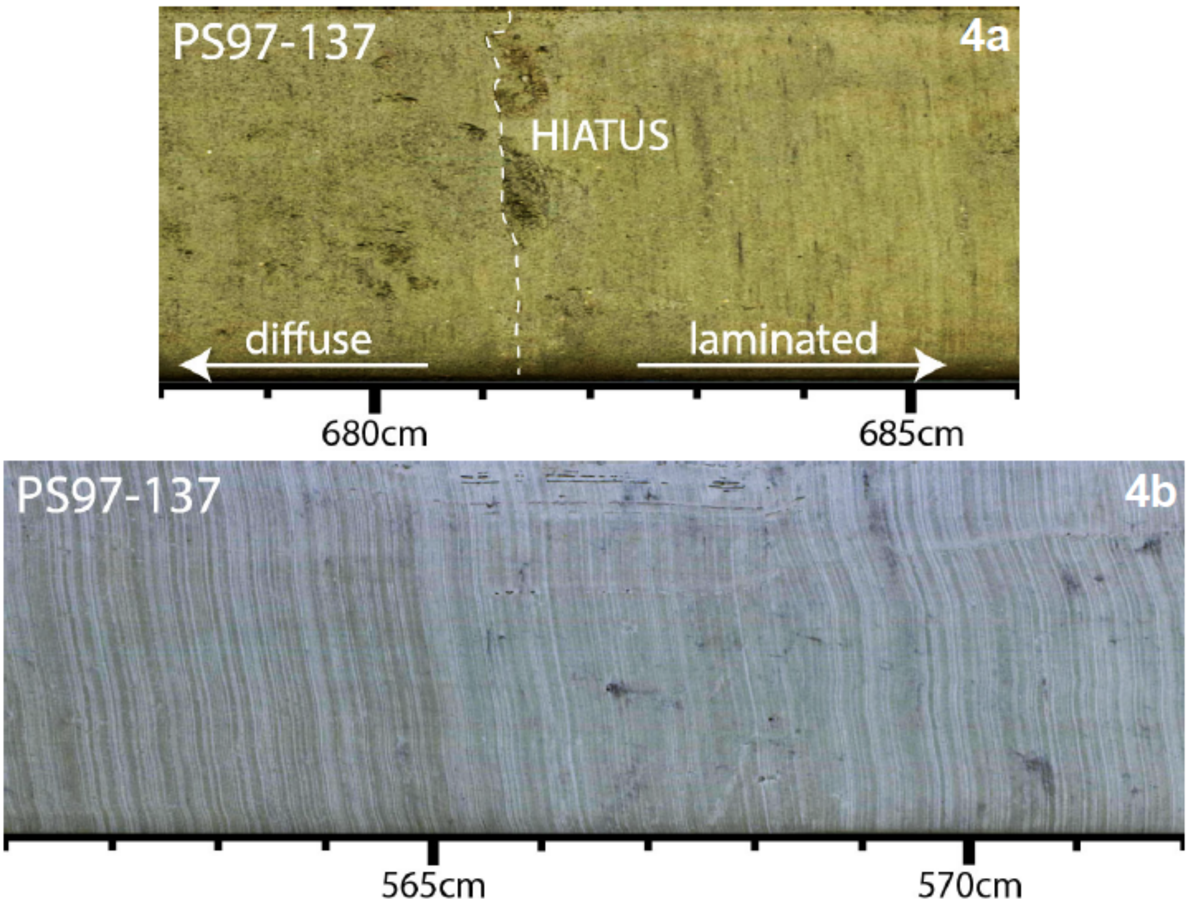

Fig. 5. Compilation of glacial-to-deglacial planktic ^{14}C reservoir ages (MRA values) estimated for four region-specific sediment cores analyzed in this study and compared to IntCal13-based mode MRA values compiled for cores from the Southern Ocean by Skinner et al. (2019).

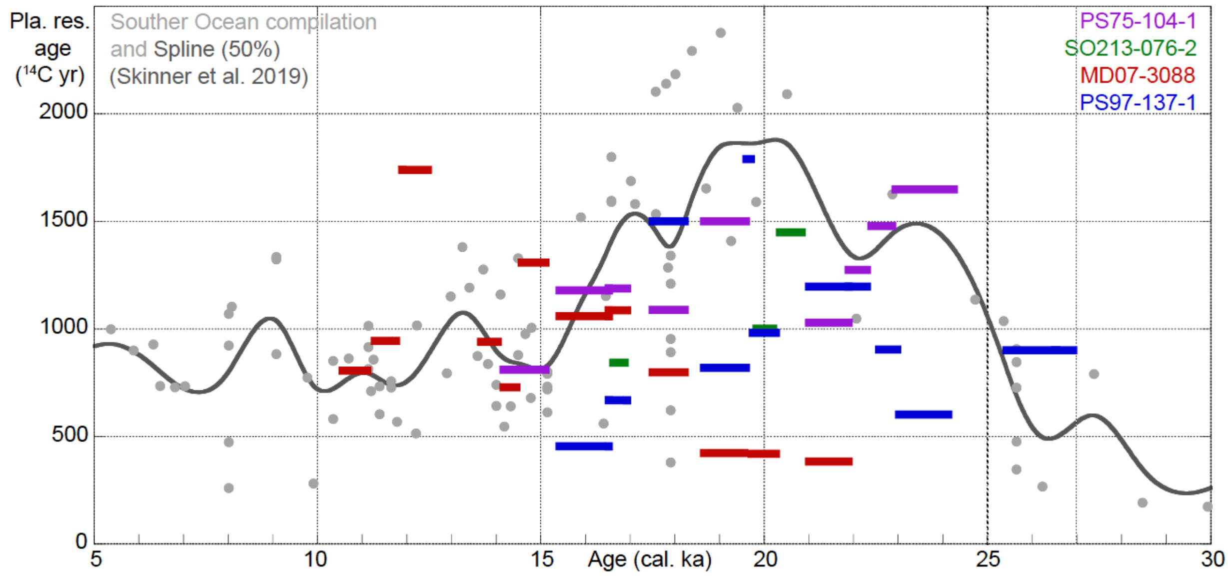

Fig. S1. Sediment laminations with a minor disconformity near 299 cm depth (= 49.5–50 cm on yardstick).

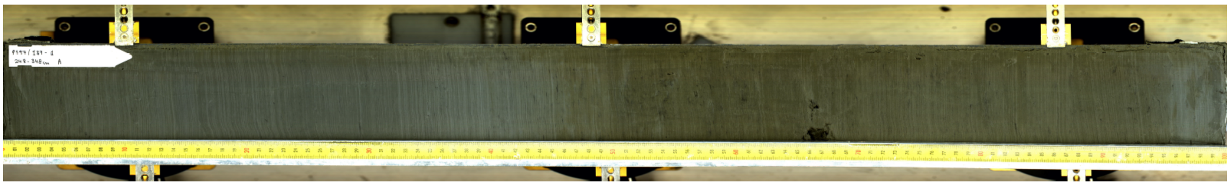

Fig. S2. Alternative mode of ^{14}C plateau tuning of paired planktic ^{14}C and $\delta^{18}O$ records of Core PS97-137-1 (for discussion see text).

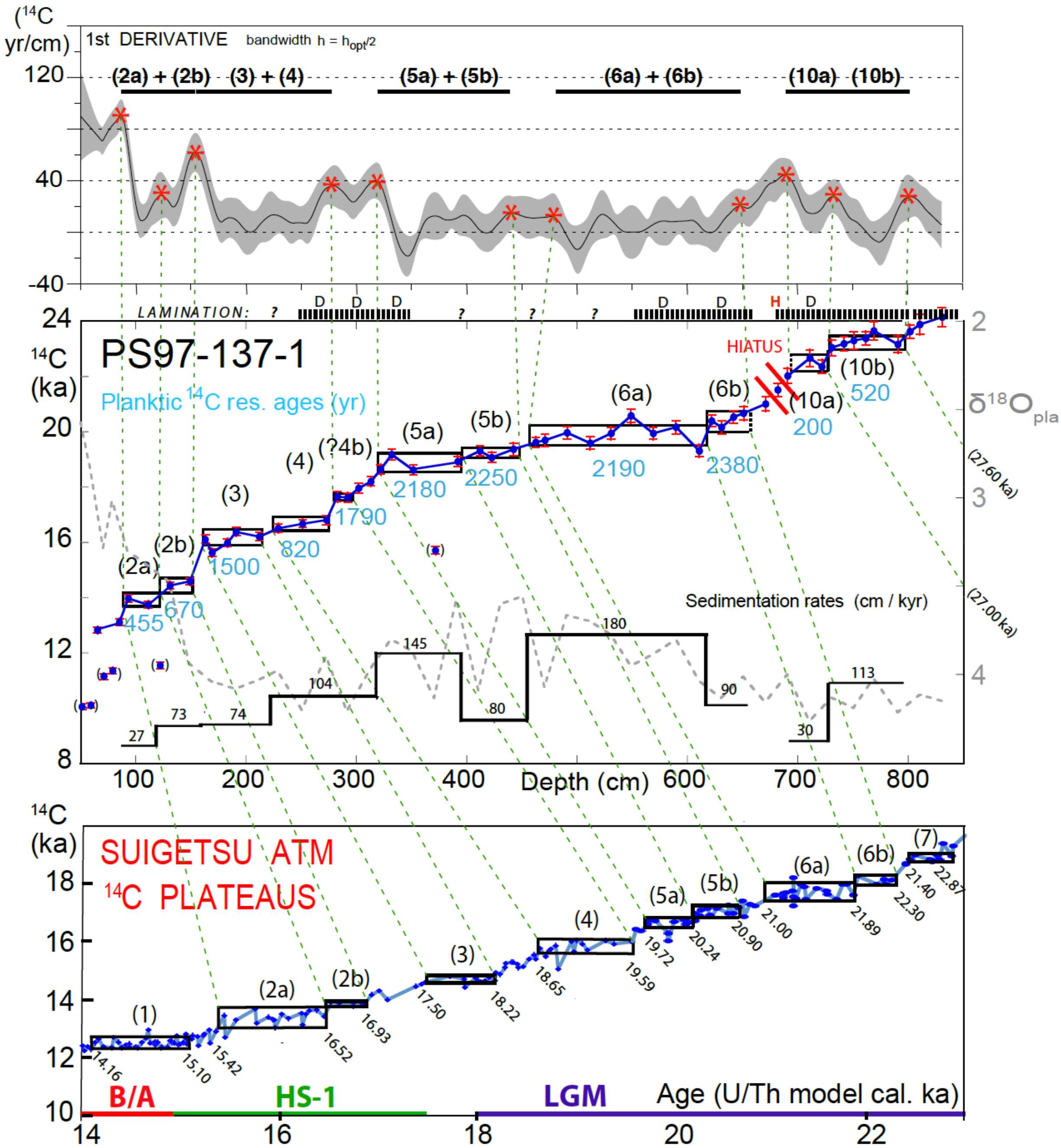

Fig. S3. Uk37-based SST and benthic $\delta^{18}O$ records of Core MD97-2120 (blue) (Pahnke et al., 2005) tuned to ^{14}C plateau-based age model for PS75-104-1 (red). Age control is compared to EDML $\delta^{18}O$ record of Antarctic temperatures and to the Liesicki & Stern (2016) stack of benthic d18O records of the intermediate Pacific.

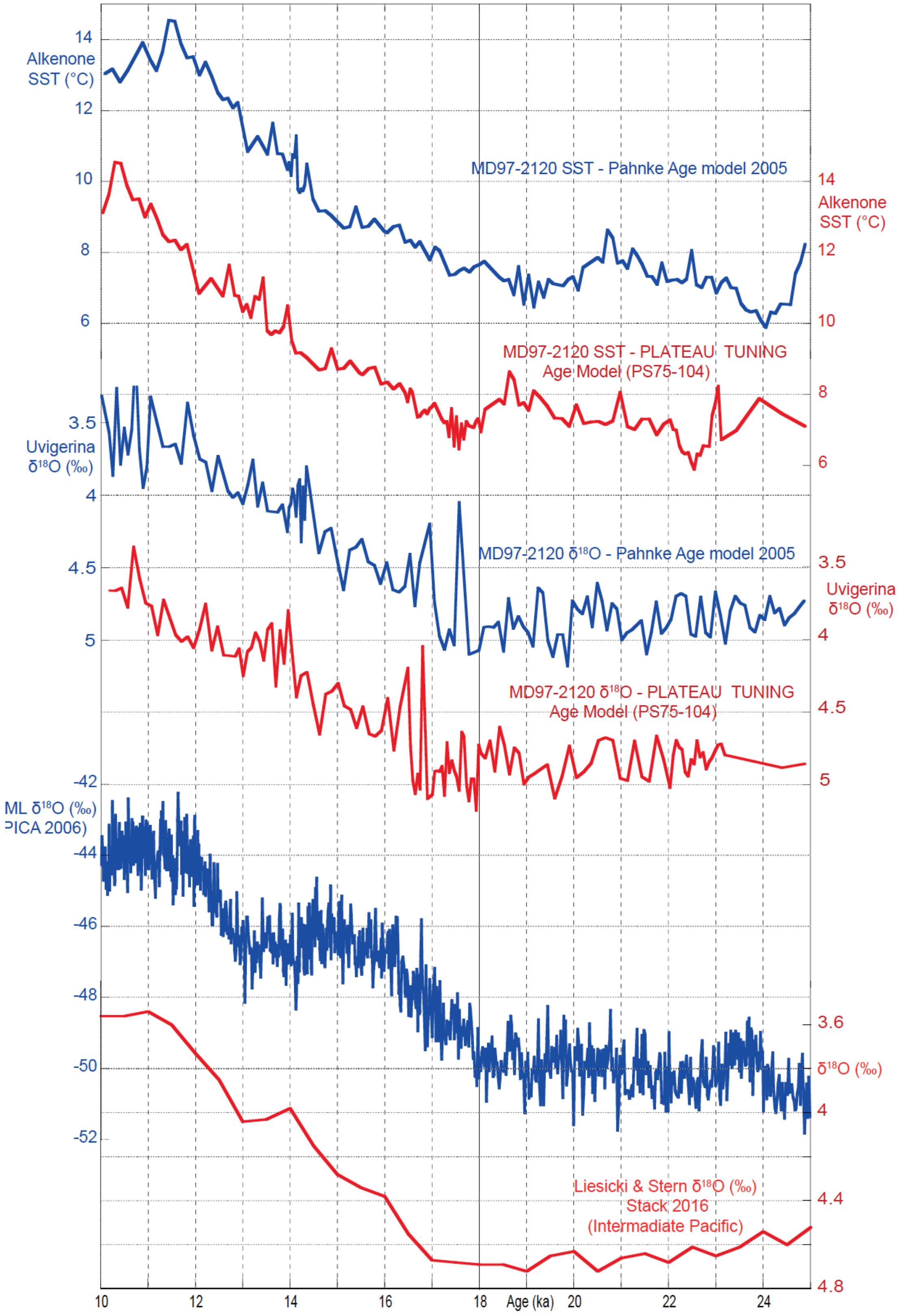

Fig. S4. Planktic ^{14}C plateaus and MRA in Core MD07-3088 versus XRF-based Ti/K data and grain sizes >63 um (Siani et al., 2013, and unpubl.data), marked by a single layer of high Ti/K ratio and enhanced fine-sand content in parallel with extreme sedimentation rates of 730 cm/ky linked to ^{14}C Plateau 5a. ACR = Antarctic cold reversal.

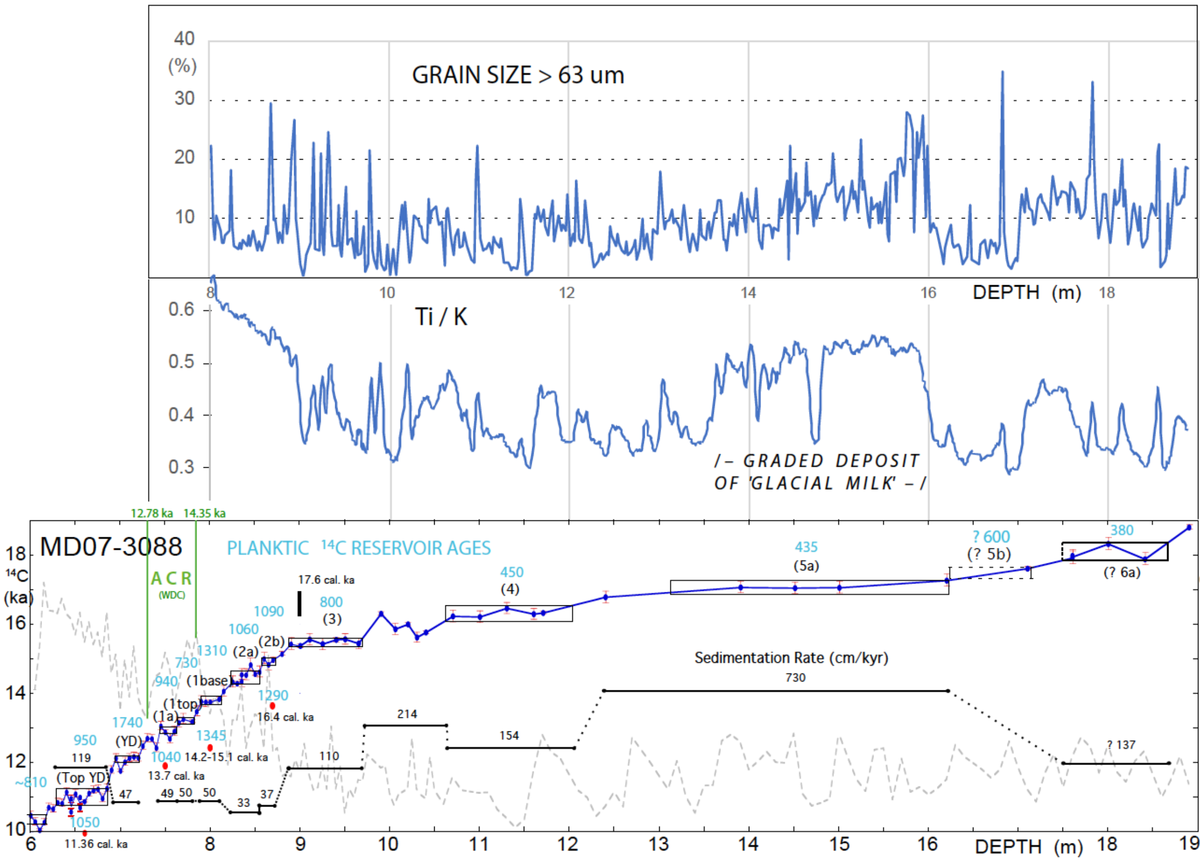

Supporting Information

Table S1- S4. Listings of ^{14}C ages and derivates for four cores presented in this paper

The contents of Suppl. Table S1-S4 are archived at **'PANGAEA'** Data Archiving and Publication (PDI-24801).